

Simone Strasser

Design, Synthesis and Characterization of Latent Ruthenium Based
Metathesis Initiators

Master Thesis

Diplomarbeit

Zur Erlangung des akademischen Grades einer Diplom-Ingenieurin
Der Studienrichtung Technische Chemie
erreicht an der Technischen Universität Graz

February 2012

Betreuer: Univ.-Doz. Dipl. Ing. Dr. techn. Christian Slugovc
Institut für Chemische Technologie und Materialien
Technische Universität Graz

Eidesstaatliche Erklärung

Room for Interpretation.

Acknowledgement

Herewith I would like to express my deep gratitude to all who helped me completing this work and who accompanied me during my studies.

I thank Christian Slugovc for supervising my master thesis, for many helpful advices and for supporting me with his excellent knowledge. Furthermore I want to thank him for giving me the opportunity to attend an international conference and a meeting within the framework of the EUMET project.

Financial support by the European Community (CP-FP 211468-2 EUMET) is gratefully acknowledged.

My gratitude also goes to Petra Kaschnitz for recording special NMR-measurements and for many useful and instructive conversations in terms of NMR-spectroscopy. In addition, I want to thank Josephine Hobisch for all the protracted and internal standard-shifting GPC-measurements. Furthermore I thank Roland Fischer and Petra Wilfling for recording X-ray crystal structures.

Of course I want to thank all my colleagues for assisting me in every need, for spending many pleasurable hours together and for an inspiring working environment day by day. Special thanks go to the members of the EUMET project at ICTM for supporting and helping me in many questions and for sharing their data and experience. It was a pleasure to be part of this wonderful work group, I spent a great time at this institute.

I express my heartfelt gratitude to Fabian for being at my side all the time. Thank you for your loving attention, for your support, for giving me the feeling of security and for keeping up your good spirits even during stressful times.

My sincere thank is owed to my family for being with me and helping me all the time, for their special care in every life situation and for their faith and trust in me. Thank you for the love I received and for offering a place where I always felt protected and comfortable.

Furthermore I want to particularly thank Fabian's family for the warm and friendly welcome in their home and for supporting me in the last years.

Abstract

The current work describes the synthesis of a series of latent ruthenium based initiators for the ring opening metathesis polymerization (ROMP) of strained cyclic olefins in general and dicyclopentadiene (DCPD) in particular. Initiator-design is aimed at obtaining solubility in neat DCPD, and achieving latent behavior at room temperature and high polymerization activity upon increasing the temperature. Initiators are composed of ruthenium as the metal center, two chloride coligands, an N-heterocyclic carbene H₂IMes (1,3-bis(2,4,6-trimethyl-phenyl)-4,5-dihydroimidazol-2-ylidene) and a chelating benzylidene carbene ligand, which is the key for obtaining the desired properties. For the benzylidene carbene precursors, a series of 5-alkoxy-4-methoxy-2-vinylbenzaldehyde derivatives (alkoxy = benzyloxy, butyloxy, hexyloxy or octyloxy) was prepared by etherification of 2-bromo-5-hydroxy-4-methoxy benzaldehyde and subsequent palladium(0) catalyzed vinylation. Those precursors were reacted with indenylidene complex **M31** (Umicore) and the corresponding complexes of the general composition *cis*-dichloro(5-alkoxy-2-formyl-4-methoxybenzylidene- $\kappa^2(C,O)$)(1,3-bis(2,4,6-trimethyl-phenyl)-4,5-dihydroimidazol-2-ylidene)ruthenium(II) were obtained. Comprehensive characterization of the complexes was done using most importantly various NMR spectroscopic techniques and single crystal X-ray structure investigations. The polymerization performance of the initiators was tested in various polymerizations of norbornene derivatives, in particular DCPD, using a related already disclosed initiator, namely *cis*-dichloro(2-formylbenzylidene- $\kappa^2(C,O)$)(1,3-bis(2,4,6-trimethyl-phenyl)-4,5-dihydroimidazol-2-ylidene)ruthenium(II) as the reference. The newly introduced initiators featuring the hexyloxy or the octyloxy substituent show increased solubility in DCPD and clearly improved latency at room temperature when compared to the reference initiator.

Kurzfassung

Diese Arbeit beschäftigt sich mit der Synthese einer Serie latenter Ruthenium-Initiatoren für die ringöffnende Metathesepolymerisation (ROMP) von gespannten zyklischen Olefinen, im speziellen von Dicyclopentadien (DCPD). Die Initiatoren sollen eine gute Löslichkeit in reinem DCPD aufweisen und außerdem latentes Verhalten bei Raumtemperatur und hohe Polymerisationsaktivität bei steigender Temperatur erreichen. Die Komplexe bestehen aus einem Ruthenium Zentralatom, zwei Chlorid-Coliganden, einem N-heterocyclischen Carben H_2IMes (1,3-bis(2,4,6-trimethyl-phenyl)-4,5-dihydro-imidazol-2-yliden), sowie einem für die gewünschten Eigenschaften entsprechend ausgestatteten chelatisierenden Benzylidenliganden. Eine Reihe solcher Benzylidenliganden (5-Alkoxy-4-methoxy-2-vinylbenzaldehydderivate; Alkoxy = Benzyloxy, Butyloxy, Hexyloxy bzw. Octyloxy) wurde durch Veretherung von 2-Bromo-5-hydroxy-4-methoxybenzaldehyd und anschließender Palladium(0) katalysierter Vinylierung synthetisiert. Um die entsprechenden Komplexe mit der allgemeinen Zusammensetzung *cis*-Dichloro(5-alkoxy-2-formyl-4-methoxybenzylidene- $\kappa^2(C,O)$)(1,3-bis(2,4,6-trimethyl-phenyl)-4,5-dihydro-imidazol-2-ylidene)ruthenium(II) zu erhalten, wurden diese mit Indenylidenkomplex **M31** (Umicore) umgesetzt. Die neuen Rutheniumkomplexe wurden mit verschiedenen NMR-Techniken sowie Röntgendiffraktometrie charakterisiert.

Um die Aktivität der Initiatoren zu evaluieren, wurden verschiedene Norbornenderivate, insbesondere DCPD, polymerisiert und mit einem geeigneten, bereits veröffentlichten Referenzinitiator (*cis*-dichloro(2-formylbenzylidene- $\kappa^2(C,O)$)(1,3-bis(2,4,6-trimethyl-phenyl)-4,5-dihydroimidazol-2-ylidene)ruthenium(II)) verglichen. Die synthetisierten Initiatoren mit Hexyloxy- bzw. Octyloxysubstituenten zeigen deutlich verbesserte Löslichkeit in DCPD und die Latenz bei Raumtemperatur ist im Vergleich zum Referenzkomplex deutlich gesteigert.

Table of Content

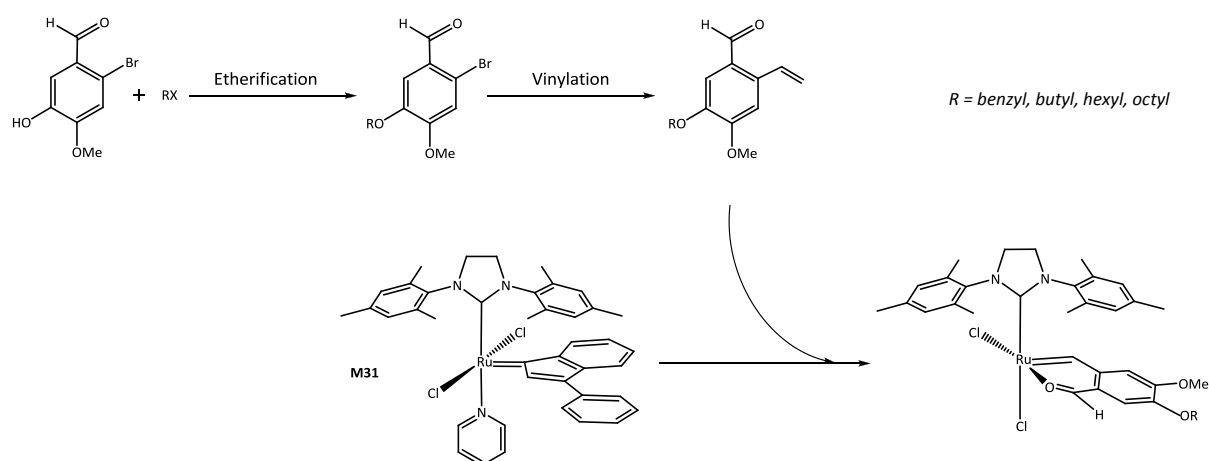
1 Introduction and Motivation.....	9
2 General Aspects.....	10
2.1 Well-defined Latent Initiators	11
2.2 ROMP of DCPD.....	13
2.3 Mechanistic Background	14
3 Results and Discussion	16
3.1 Ligands.....	17
3.2 Complexes	21
3.2.1 Synthesis.....	21
3.2.2 NMR Measurements	21
3.2.2.1 NHC Resonances.....	25
3.2.3 X-ray Structures.....	27
3.2.4 Solubility.....	30
3.2.5 Ring Opening Metathesis Polymerization (ROMP)	31
3.2.5.1 ROMP of Mon1	31
3.2.5.2 ROMP of Mon2	38
3.2.5.3 Simultaneous Thermal Analysis (STA)	43
4 Conclusion and Outlook	46
5 Experimental	48
5.1 Instruments and Materials	48
5.2 Syntheses.....	49
5.2.1 Esterifications.....	49
5.2.1.1 4-Bromo-5-formyl-2-methoxyphenyl palmitate (P5).....	49
5.2.1.2 4-Bromo-5-formyl-2-methoxyphenyl acetate (P6)	50
5.2.2 Etherifications (5-Alkoxy-2-bromo-4-methoxy benzaldehydes)	51
5.2.2.1 5-Benzyloxy-2-bromo-4-methoxy benzaldehyde.....	51
5.2.2.2 2-Bromo-5-butyloxy-4-methoxy benzaldehyde	51
5.2.2.3 2-Bromo-5-hexyloxy-4-methoxy benzaldehyde.....	52
5.2.2.4 2-Bromo-5-octyloxyoxy-4-methoxy benzaldehyde.....	53
5.2.3 Vinylations (5-Alkoxy-4-methoxy-2-vinyl benzaldehydes)	54

5.2.3.1	5-Benzyloxy-4-methoxy-2-vinyl benzaldehyde (L1)	54
5.2.3.2	5-Butyloxy-4-methoxy-2-vinyl benzaldehyde (L2)	55
5.2.3.3	5-Hexyloxy-4-methoxy-2-vinyl benzaldehyde (L3).....	56
5.2.3.4	4-Methoxy-5-octyloxy-2-vinyl benzaldehyde (L4)	57
5.2.4	Ruthenium(II) Complexes	58
5.2.4.1	Dichloro(4-benzyloxy-2-formyl-5-methoxybenzylidene- κ^2 (C,O))(1,3-bis(2,4,6-trimethylphenyl)-4,5-dihydroimidazol-2-ylidene)ruthenium (1).....	58
5.2.4.2	Dichloro(4-butyloxy-2-formyl-5-methoxybenzylidene- κ^2 (C,O))(1,3-bis(2,4,6-trimethylphenyl)-4,5-dihydroimidazol-2-ylidene)ruthenium (2).....	59
5.2.4.3	Dichloro(2-formyl-4-hexyloxy-5-methoxybenzylidene- κ^2 (C,O))(1,3-bis(2,4,6-trimethylphenyl)-4,5-dihydroimidazol-2-ylidene)ruthenium (3).....	61
5.2.4.4	Dichloro(2-formyl-5-methoxy-4-octyloxybenzylidene- κ^2 (C,O))(1,3-bis(2,4,6-trimethylphenyl)-4,5-dihydroimidazol-2-ylidene)ruthenium (4).....	62
5.2.5	Ring Opening Metathesis Polymerization (ROMP)	64
5.2.5.1	ROMP of Mon1 (M:I = 300)	64
5.2.5.2	ROMP of Mon1 in NMR tube (M:I = 10)	64
5.2.5.3	ROMP of DCPD (Mon2)	65
5.2.5.4	Simultaneous Thermal Analysis (STA)	65
Appendix.....		66
List of Abbreviations		66
List of Figures		67
List of Schemes		68
List of Tables		69

1 Introduction and Motivation

The scope of this work was the synthesis and characterization of novel latent second generation dichloro ruthenium initiators bearing chelating ligands, so called 5-alkoxy-4-methoxy-2-vinyl benzaldehydes (see Scheme 1). A vinyl derivative bearing an aldehyde functionality as chelating moiety was chosen due to the promising applicability for ROMP of DCPD. However, a limiting property of these compounds is the poor solubility in nonpolar media.

Therefore, the alkoxy residue was introduced to increase the solubility of the complexes in nonpolar substances, such as DCPD to enable a solvent free processing. The complexes were tested in ROMP, firstly to characterize the polymerization activity and secondly, to show a trend between solubility and performance.



Scheme 1. General reaction scheme for the synthesis of dichloro-ruthenium complexes

In respect of the appearance of unexpected carbene species, more intense studies became necessary. Particularly interesting was the difference between the benzyl and the butyl derivative, which should be investigated more detailed. To highlight and explain these differences, NMR spectroscopy, gel permeation chromatography (GPC) and X-ray diffraction crystallography were used. The received results allow a statement about the active species in the catalytic pathway and the association of solubility and performance in ROMP.

2 General Aspects

In recent years the development of ruthenium-based olefin metathesis has had an enormous impact on organic synthesis and polymer chemistry due to its versatile applicability. In particular ruthenium-based homogeneous initiators have been described in detail due to their remarkable tolerance to moisture and oxygen as well as their functional group tolerance. The variety of metathesis reaction types and reaction conditions induced a huge number of tailor-made catalyst designs with fine-tuned properties.^{1,2}

Accordingly, a broad variety of ruthenium-based initiators with diverse ligands have been developed to receive a sophisticated balance between stability and activity. However, most olefin metathesis reactions are performed with the commercially available initiators Grubbs 1st, 2nd and 3rd generation (**G1**, **G2**, **G3**), Hoveyda 2nd generation (**H2**) or **M2** and **M31** featuring an indenylidene instead of the benzylidene ligand (see Figure 1).

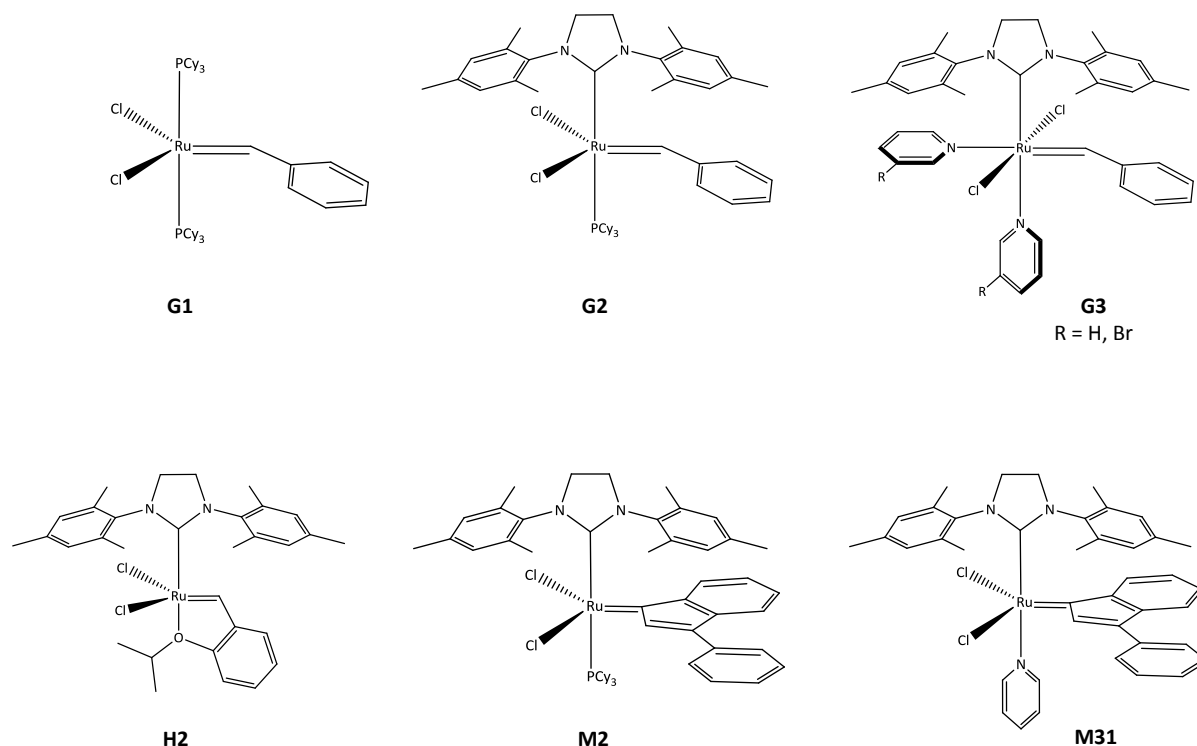


Figure 1. Most prominent commercially available initiators used in olefin metathesis

¹ D. M. Hudson, E. J. Valente, J. Schachner, M. Limbach, K. Müller, H.-J. Schanz, *ChemCatChem* **2011**, *3*, 297-301

² C. Lexer, D. Burtcher, B. Perner, E. Tzur, N.G. Lemcoff, C. Slugovc, *Journal of Organometallic Chemistry* **2011**, *696*, 2466-2470

All these compounds typically exhibit catalytic activity at room temperature. However, for particular applications and synthetic challenges, high thermal stability and thermal switchability is desired. For that purpose latent initiators have been developed.²

2.1 Well-defined Latent Initiators

A major deficiency of early ill-defined catalyst systems, such as $\text{Ru}(\text{H}_2\text{O})_6(\text{tos})_2$, is their lack of initiation efficiency which results in broad molecular weight distributions of the obtained polymers. Thus, polymerizations performed using ill-defined catalysts can not be dedicated as living. Further the need for high catalyst loadings is also limiting commercial applications. However, the advent of well-defined, highly active ruthenium catalysts and the fact that they were commercially available, urged the development of latent catalysts incorporating a ruthenium alkylidene motif. Different approaches towards the design of well-defined latent initiators are presented in Figure 2.³

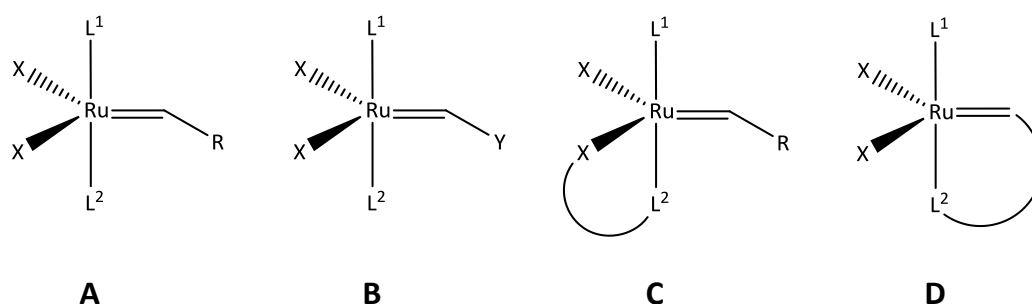


Figure 2. Well-defined latent initiators

A first category of catalysts retain the classic morphology of Grubbs' first and second generation catalysts (Figure 2, **A**). Class **B** includes complexes bearing Fischer Carbenes, which have to be activated thermally or photochemically, otherwise they show no catalytic activity. Complexes of class **C** open the coordination site by dissociation of L². Limiting is the competitive coordination between the dangling ligand and the olefinic substrate implies a

³ S. Monsaert, A. L. Vila, R. Drozdak, P. Van Der Poort and F. Verpoort, *Chem. Soc. Rev.* **2009**, *38*, 3360-3372

reduction of propagation speed. This competition is avoided when using initiators with motif D.³ The title compounds of this work can also be counted among this class of complexes.

The chemistry of transition metal complexes with chelating ligands containing mixed functionalities gains growing popularity, as the different features give unique reactivity to the metal complexes.⁴ Although application of the introduced initiators exhibits notable advantages for certain applications, efforts were directed towards the exploration of different initiator designs which are more diversified whereas the use of hemilabile chelating ligands is of major importance.³

Hemilabile ligands have the ability to place two or more donor atoms with different electronic properties close to the metal atom. They can reversibly create or occupy a vacant coordination site at the metal, with consequent stabilization of reactive intermediates or enhancement of reactivity in catalytic pathways. These ligands act as chelating moieties at room temperature and will liberate one coordination site of a competing substrate at elevated temperatures.⁴ Furthermore, steric and electronic properties of these ligands are easily varied over a wide range by the proper choice of the constituting coordinating groups, thus allowing for advanced fine-tuning of the characteristics of the precatalyst.³

A successful design motif for latent initiators is the use of a chelating carbene ligand similar to the one used in Hoveyda type complexes (see Figure 1) with strongly coordinating co-ligands using O, N, P, S and Se donor atoms at the second binding unit.²

In this contribution, an aldehyde functionality was chosen as chelating carbene ligand besides the great diversity of possible systems. This type of ruthenium complex is considered to be well suited for ring opening metathesis polymerization (ROMP) of dicyclopentadiene (DCPD).

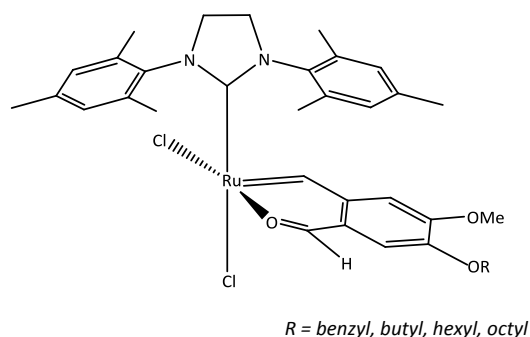
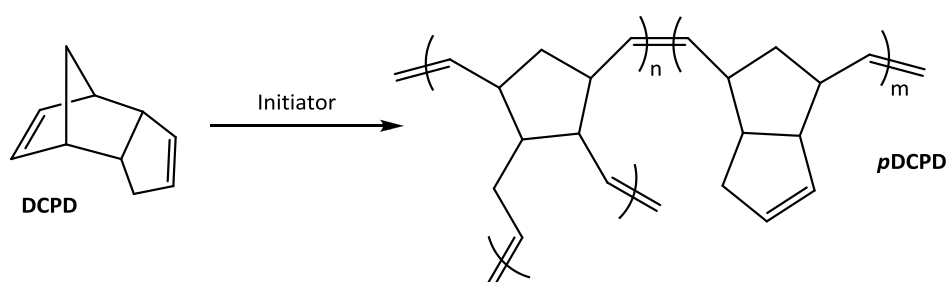


Figure 3. Chelating carbene ligand in the synthesized ruthenium complexes

⁴ R. Drozdak, N. Nishioka, G. Recher, F. Verpoort, *Macromol. Symp.* **2010**, 293, 1-4

2.2 ROMP of DCPD

Bulk ROMP of DCPD (Scheme 2) is one of the major applications of olefin metathesis initiators, as *p*DCPD represents a material of outstanding mechanical properties. Its strength is based on the high degree of cross-linking, which is a result of the secondary ROMP reaction of the unsaturated five-membered ring of linear *p*DCPD at elevated temperatures achieved under adiabatic conditions.¹ Therefore the development of tailor-made initiators for ROMP of DCPD is of high interest.



Scheme 2. Ring opening metathesis polymerization of DCPD

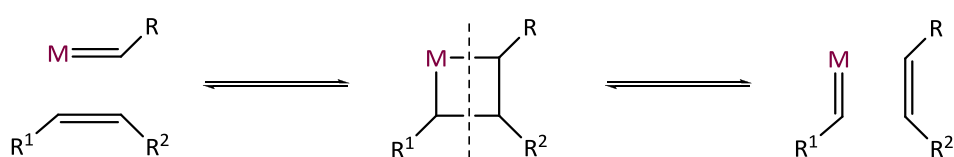
A number of latent ruthenium carbene systems with hemilabile ligands for application in ROMP of DCPD are already known. Thus bidentate O,N-chelated Schiff base⁵ containing initiators have been reported by Grubbs and later Verpoort et al. These initiators were shown to be extremely inactive towards polymerization of DCPD (and other cyclic olefins) at room temperature and have to be activated by the addition of Bronsted acids, e.g. HCl. Such systems are of high interest for reaction injection moulding processes where initiator and monomer can be stored together while a second monomer stream contains acid to start the polymerization.⁴

However, the mixing of initiator and monomer poses a technical problem, as the highly exothermic reaction may start instantly or only after a short delay period. The use of latent olefin metathesis catalysts allows for safe mixing of these compounds and ideally the mixture would have an infinite shelf life before external activation.¹

⁵ M. Jordaan, H.C. Vosloo, *Adv. Synth. Catal.* **2007**, 349, 184-192

2.3 Mechanistic Background

In this part, the basic mechanism will be explained for a better understanding of the olefin metathesis reaction. After many investigations Chauvin⁶ proposed a mechanism for olefin metathesis using transition metals in 1973, supported by numerous experimental observations⁷, which remains valid until today. Scheme 3 demonstrates the Chauvin mechanism, where a metallacyclobutane is formed from an initial carbene reacting with an incoming alkene. Cleavage yields a new alkene and a different carbene.⁸



Scheme 3. Mechanism of transition metal olefin metathesis

Starting the catalytic pathway, two possible scenarios are proposed: a dissociative and an associative mechanism for the coordination of the alkene substrate.

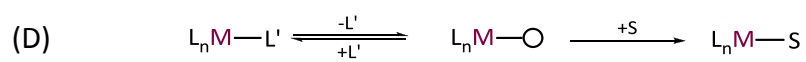
The dissociative way involves a slow initial loss of a ligand to generate a vacant site at the metal, which is trapped by the incoming substrate. The rate-determining step in this pathway is the dissociation of the ligand (Scheme 4, D). This path tends to be observed for 18 electron complexes because the alternative, associative way would generate a 20 electron species which would be energetically disadvantaged.

The associative mechanism implies the attack of the incoming substrate as the first, rate-determining step. The formed intermediate rapidly expels one of the ligands L (Scheme 4, A). This mechanism is often passed by 16 electron complexes due to a 18 electron intermediate which is preferred to the high energy 14 electron intermediate that would be formed in dissociative substitution.⁸

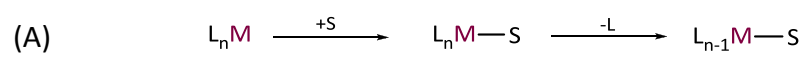
⁶ J.L. Hèrrisson, Y. Chauvin, *Makromol. Chem.* **1971**, 141, 161

⁷ R.H. Grubbs, D.D. Carr, C. Hoppin, P.L. Burk, *J. Am. Chem. Soc.* **1976**, 3478-3483

⁸ Robert H. Crabtree, *The organometallic chemistry of the transition metals*, John Wiley & Sons, Inc. New Jersey **2005**



 **ROMP**



Scheme 4. Dissociative (D) and associative (A) pathway for coordination of the alkene substrate (S)

3 Results and Discussion

The aim of this work was to synthesize new ruthenium initiators carrying chelating carbene ligands. Various ligands of this type are known and well defined, such as aldehydes⁹, ethers¹⁰, esters¹, phosphines¹¹, quinolines¹², enamines¹³ or sulphides¹⁴.

Many investigations have been done in the last years to design a latent initiator system especially for the ring opening metathesis polymerization¹⁵ (ROMP) of dicyclopentadiene (DCPD). DCPD has been established recently as a promising monomer for the manufacturing of polymers with particular material demands for highly specific applications. The great benefits of DCPD are the cheap availability and the excellent material characteristic when properly processed.

Latency is one of the major requirements of the initiator, thus it enables a mixing of initiator and monomer without contemporaneous gelation.⁴ The attempt of this work was to realize firstly the demand of latency and secondly a solvent free processing of DCPD with a new ruthenium system carrying an aldehyde moiety as chelating ligand. To facilitate the handling of such initiator systems, a slow initiation as well as a constant propagation has to be achieved.

In order to enhance this type of initiators for the solvent free processing of DCPD, the chelating ligand was modified to increase the solubility of the complexes in this promising monomer. The modification was realized by substitution with *OR*-groups whereas *R* should be preferably nonpolar moieties like long alkyl chains.

⁹ C. Slugovc, B. Perner, F. Stelzer, K. Mereiter, *Organometallics* **2004**, *23*, 3622-3626

¹⁰ J.S. Kingsbury, J.P.A. Hatrriy, A.H. Hoveyda, *J. Am. Chem. Soc.* **1999**, *121*, 791

¹¹ B. Perner, *Thermally Switchable Initiators for Ring Opening Metathesis Polymerisation*, Diploma Thesis, Graz, **2004**

¹² X. Gstrein, D. Burtscher, A. Szadkowska, M. Barbasiewicz, F. Stelzer, K. Grela, C. Slugovc, *Journal of Polymer Science: Part A: Polymer Chemistry* **2007**, *45*, 3494-3500

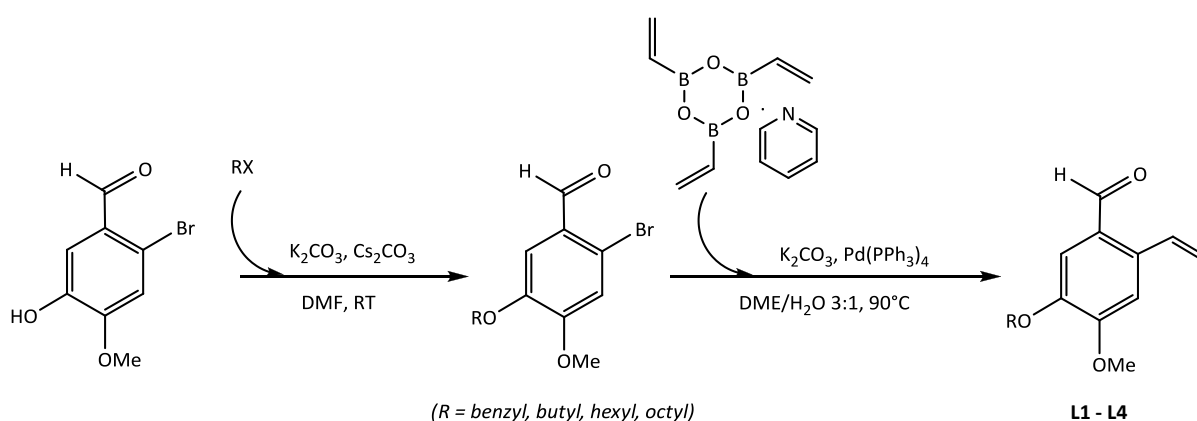
¹³ C. Slugovc, D. Burtscher, K. Mereiter, F. Stelzer, *Organometallics* **2005**, *24*, 2255

¹⁴ A. Ben-Asuly, E. Tzur, C.E. Diesendruck, M. Sigalov, I. Goldberg, N.G. Lemcoff, *Organometallics* **2008**, *27*, 811-813

¹⁵ A. Leitgeb, J. Wappel and C. Slugovc, *Polymer* **2010**, *51*, 2927

3.1 Ligands

The preparation of the new ligands is a straight forward two-step synthesis (see Scheme 5), using already established routes. In the first step different residues were introduced via etherification¹⁶ of the hydroxy group of a commercially available substituted benzaldehyde. Therefore, 2-bromo-5-hydroxy-4-methoxybenzaldehyde was reacted with the appropriate alkyl halide under basic conditions in dimethylformamide at room temperature for 20 h. Yields ranged from 73-83 % after purification via column chromatography or recrystallization.



Scheme 5. Two-step synthesis for the preparation of ligands **L1-L4**

First, a protocol from Chandrasekhar et al was followed.¹⁷ While stirring for 3 days at rather harsh reaction conditions (65°C, alkaline), an intramolecular reaction at the aldehyde moiety through reaction with the solvent acetone took place. The side product was isolated and identified by NMR analysis and turned out to have a structure as depicted in Figure 4. In the following the procedure was modified to avoid these side reactions and enhance yield. Acetone was replaced by dimethylformamide, Cs₂CO₃ was used additionally as base and reactions were carried out at room temperature instead (see Scheme 5). Thus the above mentioned side reaction was prohibited and a yield of >90 % can be reported.

¹⁶ A. Leitgeb, A. Szadkowska, M. Michalak, M. Barbasiewicz, K. Grela, C. Slugovc, *J. Polym. Sci. Part A: Polym. Chem.* **2011**, *49*, 3448-3454

¹⁷ S. Chandrasekhar et al., *Tetrahedron* **2006**, *62*, 12104-12105

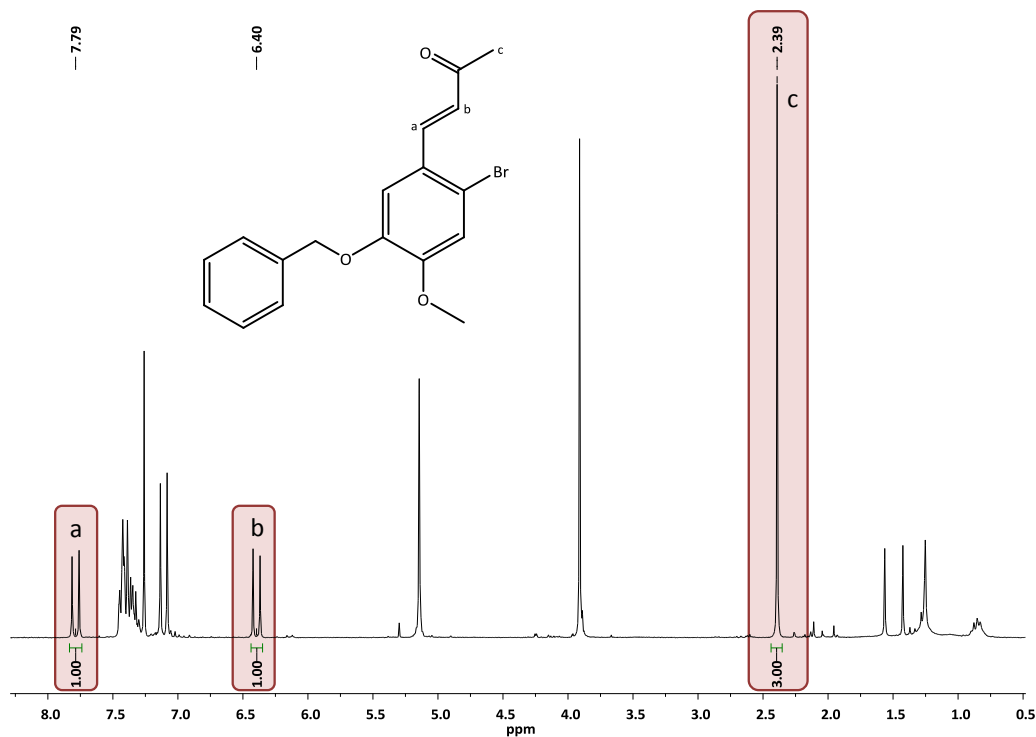


Figure 4. ¹H NMR spectrum of the side product (300 MHz, CDCl₃)

In the second step the desired compounds were reached by vinylation via Suzuki-Miyaura cross-coupling.⁹ Therefore 2,4,6-trivinylcyclotriboroxane anhydride pyridine complex and catalytic amounts of Pd(PPh₃)₄ (3 mol%) were used in the presence of K₂CO₃. The Suzuki-coupling is considered to be the limiting step in this synthesis due to the rather harsh reaction conditions (basic solution, 90°C, 30 h). Yields of the purified compounds were 75 - 90 %. More details are listed in the experimental section (chapter 5.2.3). A characteristic ¹H NMR spectrum of a vinyl compound is depicted in Figure 5.

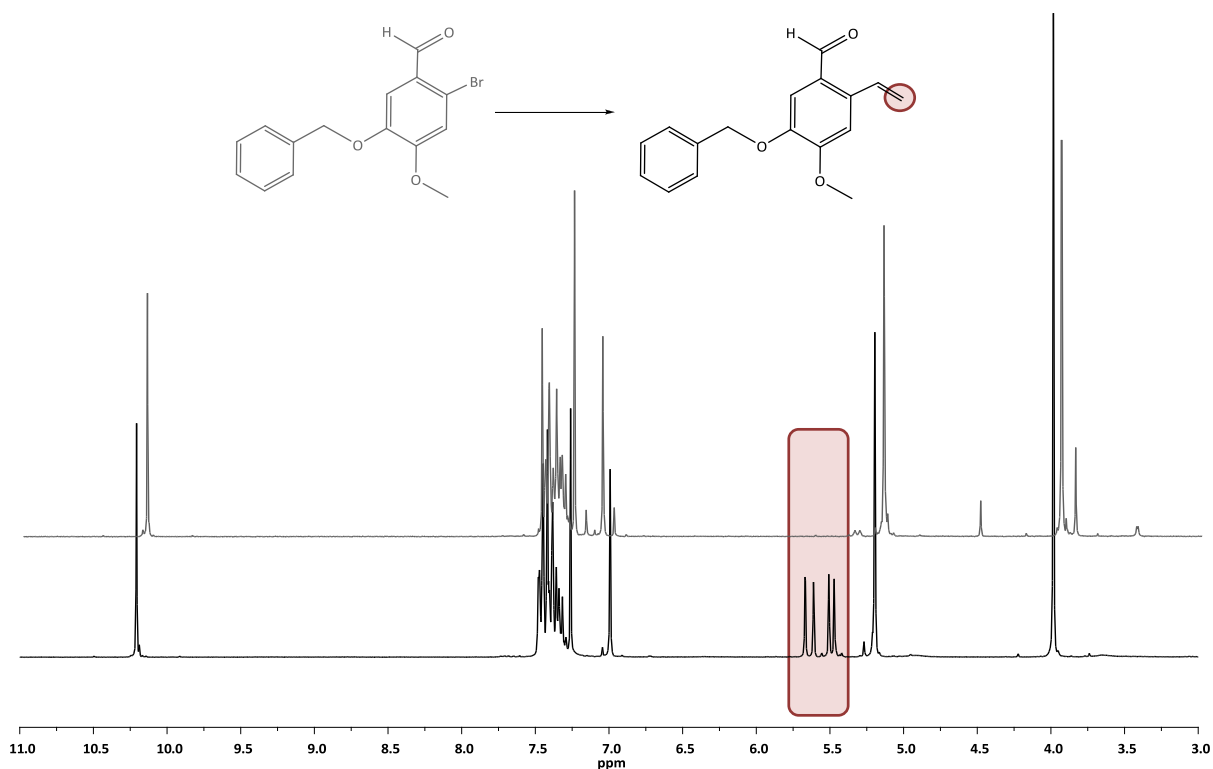


Figure 5. Characteristic ^1H NMR spectrum of a vinyl compound (**L1**, 300 MHz, CDCl_3)

An alternative pathway to obtain ligands, carrying alkyl side chains was explored by introducing different acid chlorides via esterification¹⁸. The compounds **P5** and **P6** (Table 2) could be obtained in moderate yields (40 % after column chromatography), but the ester group turned out to be not stable during the following vinylation. Obviously, the ester functionality in *para* position to the bromide is not as stable as in *ortho* position.

To avoid decomposition of the ester group within the Suzuki-coupling, the vinyl group was introduced in the first reaction step. Unfortunately, vinylation of 2-bromo-5-hydroxy-4-methoxybenzaldehyde failed under these conditions,¹ presumably due to a positive mesomeric effect of the hydroxy group in *para* position to the bromide. With this knowledge the focus was laid on the etherification and the subsequent optimization of the reaction conditions to achieve good yields.

¹⁸ E. Pump, Olefin Metathesis with *cis*-Dichloro Ruthenium Benzylidene Complexes: *New Mechanistic Insights*, Master Thesis, **2011**

Table 1. Ligands used for initiator synthesis

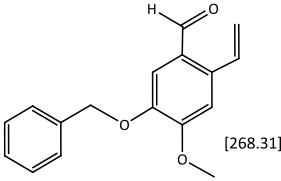
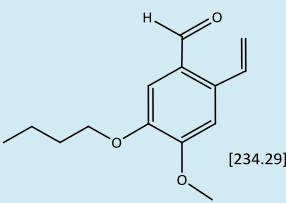
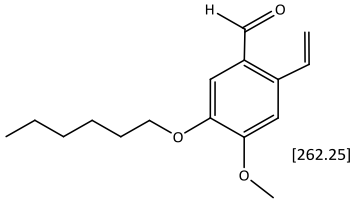
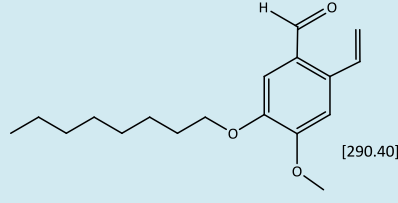
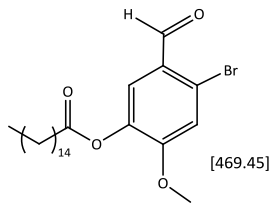
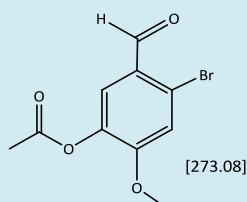
L1	 [268.31]	5-Benzoyloxy-4-methoxy-2-vinyl benzaldehyde
L2	 [234.29]	5-Butyloxy-4-methoxy-2-vinyl benzaldehyde
L3	 [262.25]	5-Hexyloxy-4-methoxy-2-vinyl benzaldehyde
L4	 [290.40]	5-Octyloxy-4-methoxy-2-vinyl benzaldehyde

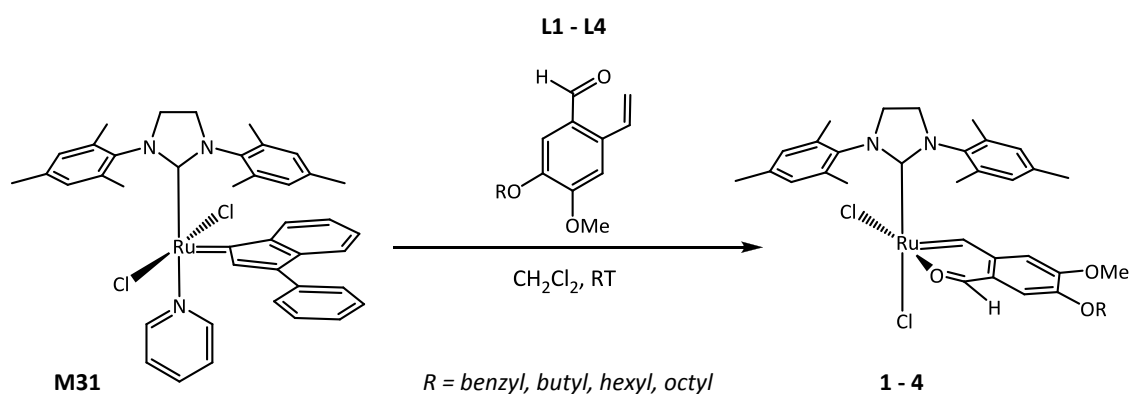
Table 2. Esters (ligand precursors)

P5	 [469.45]	4-Bromo-5-formyl-2-methoxyphenyl palmitate
P6	 [273.08]	4-Bromo-5-formyl-2-methoxyphenyl acetate

3.2 Complexes

3.2.1 Synthesis

The ruthenium initiators were prepared by a carbene exchange reaction of **M31** with the above mentioned vinyl derivatives **L1-L4** (Table 1) according to literature (see Scheme 6).⁹ **M31** has been established as good starting material for the preparation of *cis*-dichloro ruthenium complexes bearing chelating carbenes.¹⁸



Scheme 6. Synthesis of ruthenium complexes **1-4** starting from **M31** ([1,3-bis(2,4,6-trimethylphenyl)-2-imidazolidinylidene]dichloro(3-phenyl-1H-inden-1-ylidene)(pyridyl)ruthenium(II))

A mixture of **M31** (1 eq) and 5-alkoxy-4-methoxy-2-vinyl benzaldehyde (1.15 eq) was stirred in dry degassed CH_2Cl_2 at room temperature until the mixture turned from deep red to deep green and full conversion was detected by TLC. The complexes were isolated as green powder by precipitation upon addition of *n*-pentane and subsequent column chromatography in moderate yields (approx. 65 %).

3.2.2 NMR Measurements

^1H NMR spectra (see Figure 6) of the crude complexes exhibited the presence of two carbene species in a 4:1 ratio. Column chromatography ($\text{CH}_2\text{Cl}_2/\text{MeOH}$, 10:1, (v:v)) allowed their separation and the main fraction (carbene proton resonances between 18.40 and 18.50 ppm) was identified as *cis*-dichloro complex by ^1H NMR, ^{13}C NMR and X-ray diffraction analysis.

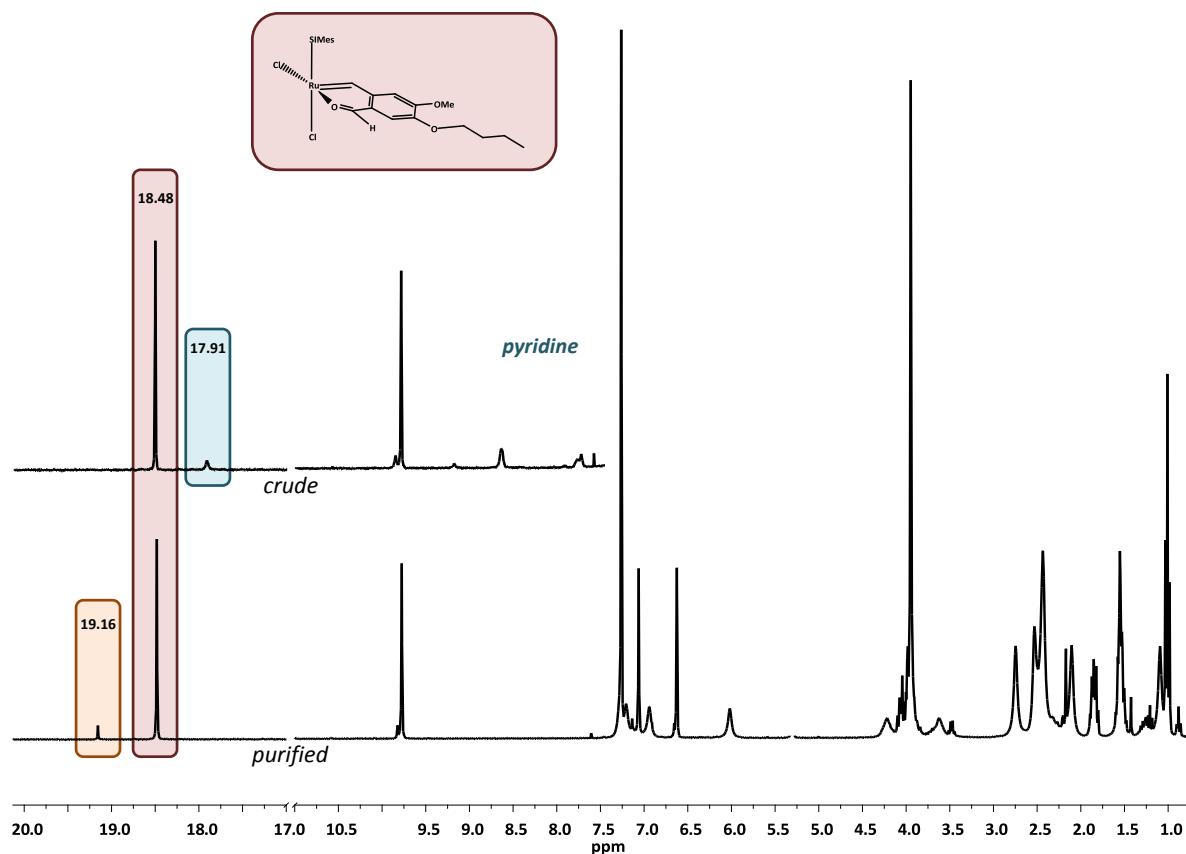


Figure 6. ^1H NMR spectra of complex **2** (300 MHz, CDCl_3)

The side product was identified as a cationic pyridine adduct by ^1H NMR analysis. Although the molecular structure was not obtained by X-ray diffraction, the signals at 8.59 ppm (d), 7.76 ppm (t) and 7.33 ppm (dd) are characteristic for a pyridine coordination (Figure 7).¹⁹ Another interesting observation is the decoordination of the N-heterocyclic carbene ligand (NHC, H_2IMes), which happens most likely during the purification of **2** via column chromatography ($\text{CH}_2\text{Cl}_2/\text{MeOH}$, 10:1, (v:v)). The H_2IMes ligand eluates within the later fractions and shows characteristic singlet signals at 9.33, 6.90, 4.54, 2.35 and 2.23 ppm. These signals are crossed out for better clarity in Figure 7.

¹⁹ M. Zirngast, E. Pump, A. Leitgeb, J. H. Albering, C. Slugovc, *Chem. Commun.* **2011**, 47, 2261-2263

* H_2IMes = 1,3-bis(mesityl)-4,5-dihydroimidazol-2-ylidene (NHC)

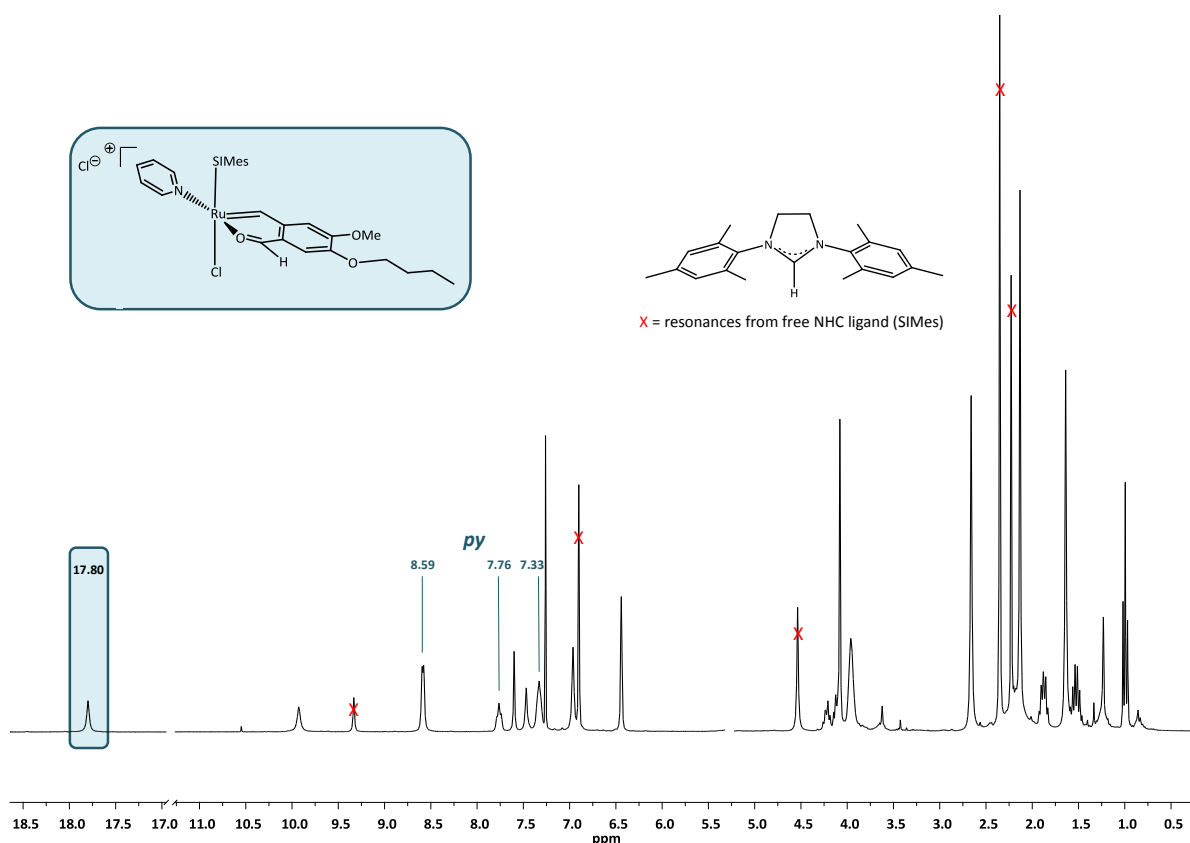


Figure 7. ^1H NMR spectrum of the cationic side product (**2a**) (300 MHz, CDCl_3)

A third carbene proton resonance appears at 19.16 ppm after purification by column chromatography within the main fraction in a 10:1 ratio for complexes **2**, **3**, and **4** (see Figure 6). For complex **1**, this carbene signal occurred only in a 3 % proportion and decomposed completely after 6 days. Although separation of the two species was not feasible, further NMR measurements and have been done to receive more structural information about this complex. The fact that this compound appeared only after purification with a methanol-containing eluent is a hint for an interaction between the solvent and the Ru-complex. Therefore ^1H and advanced NMR spectra (NOESY, HSQC) were recorded in methanol- d_4 . (see Figure 8). However, these measurements were not practicable due to limited solubility of the complex in methanol. A further difficulty arose in the low stability of the complex in methanol which disabled crystal growth.

The first presumption reflecting the resonances appearing in methanol- d_4 was the existence of a *trans*-dichloro species. But a more precise look exhibited a diastereotopic splitting for the protons vicinal to the oxygen in the butyloxy residue (highlighted in Figure 8). This pattern would not occur if the complex possesses a *trans*-dichloro structure. In this case

these two protons would appear as one triplet, because the mesityl moiety of the H₂IMes ligand would be too far off to affect them magnetically.

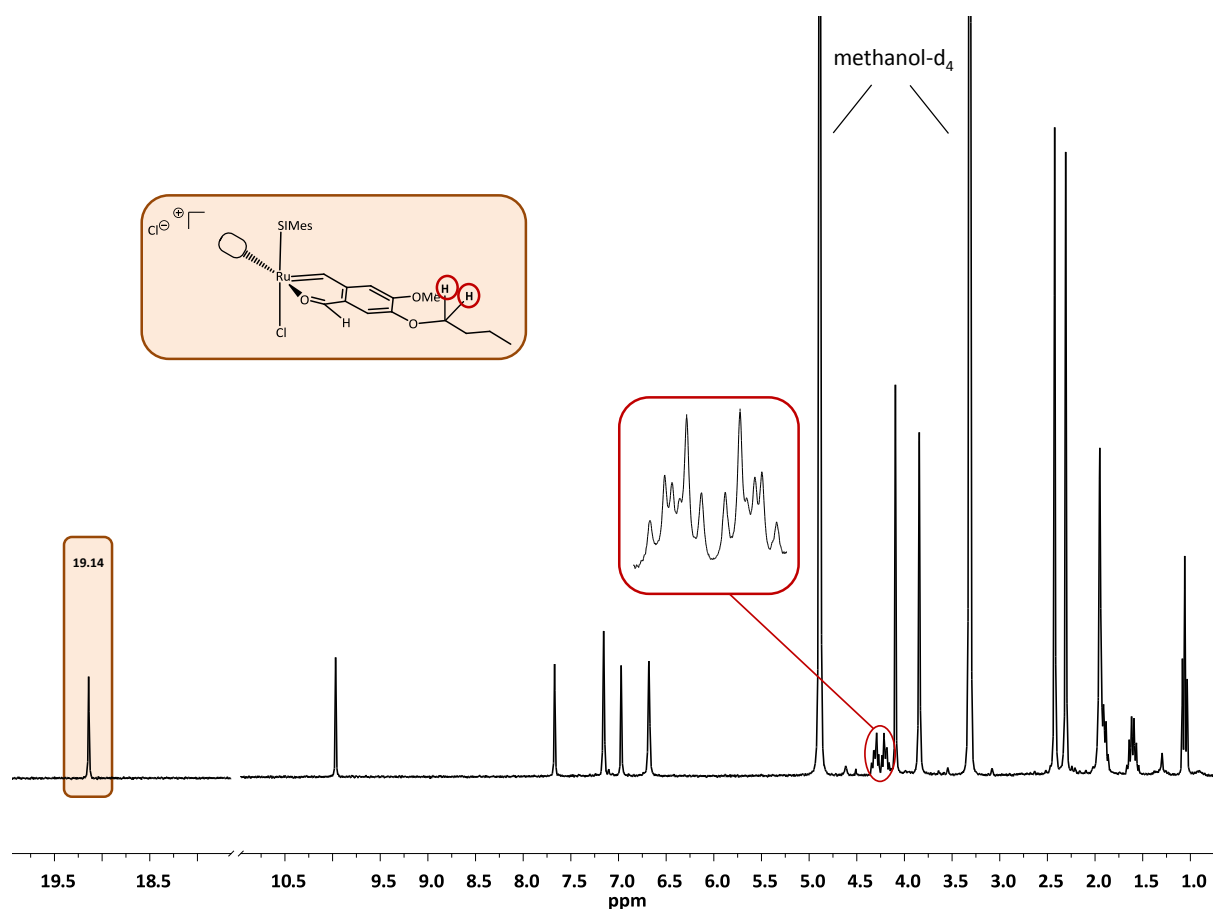
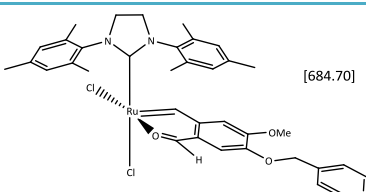
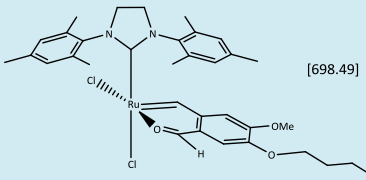
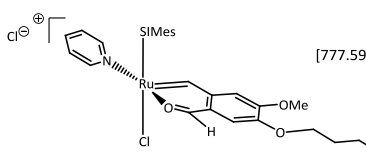
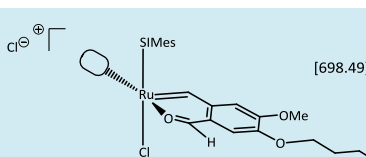
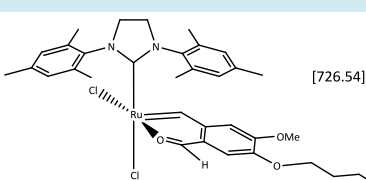
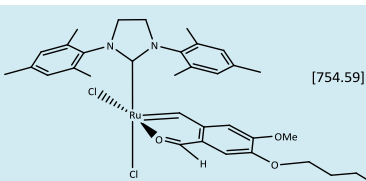


Figure 8. ¹H NMR spectrum of complex **2b** (300.36 MHz, methanol-d₄)

The information received through NMR spectroscopy and the results of conducted ROMP experiments within this work (see chapter 3.2.5), suggest that the complexes under investigation exist as a cationic species in methanol-d₄ as already stated for *cis*-dichloro ruthenium benzylidenes bearing an ester functionality. It has been observed that this cationic species is an intermediate in the rearrangement of the *cis*-dichloro complexes to their catalytically active *trans*-dichloro analogues.¹⁹

Table 3. *Cis*-dichloro ruthenium complexes

1	 [684.70]	Dichloro(2-formyl-4-benzyloxy-5-methoxybenzylidene- $\kappa^2(C,O)$)(1,3-bis(2,4,6-trimethylphenyl)-4,5-dihydroimidazol-2-ylidene)ruthenium
2	 [698.49]	Dichloro(2-formyl-4-butyloxy-5-methoxybenzylidene- $\kappa^2(C,O)$)(1,3-bis(2,4,6-trimethylphenyl)-4,5-dihydroimidazol-2-ylidene)ruthenium
2a	 [777.59]	[(2-Formyl-4-butyloxy-5-methoxybenzylidene- $\kappa^2(C,O)$)-(pyridine)-(1,3-bis(2,4,6-trimethylphenyl)-4,5-dihydroimidazol-2-ylidene)ruthenium]chloride
2b	 [698.49]	[(2-Formyl-4-butyloxy-5-methoxybenzylidene- $\kappa^2(C,O)$)(1,3-bis(2,4,6-trimethylphenyl)-4,5-dihydroimidazol-2-ylidene)ruthenium]chloride*
3	 [726.54]	Dichloro(2-formyl-4-hexyloxy-5-methoxybenzylidene- $\kappa^2(C,O)$)(1,3-bis(2,4,6-trimethylphenyl)-4,5-dihydroimidazol-2-ylidene)ruthenium
4	 [754.59]	Dichloro(2-formyl-4-octyloxy-5-methoxybenzylidene- $\kappa^2(C,O)$)(1,3-bis(2,4,6-trimethylphenyl)-4,5-dihydroimidazol-2-ylidene)ruthenium

* not isolated

3.2.2.1 NHC Resonances

Depending on the conformation of the ligands coordinated to the ruthenium center, the NHC ligand shows a different signal pattern. The H₂IMes protons of a cationic species split into a different signal pattern compared to those of neutral complexes (Figure 10). An explanation for this phenomenon is the faster rotation of the Ru-C(1) bond and thus a recovery of symmetry.⁹

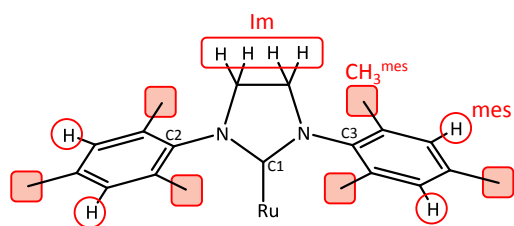


Figure 9. NHC ligand (H_2IMes) with highlighted protons

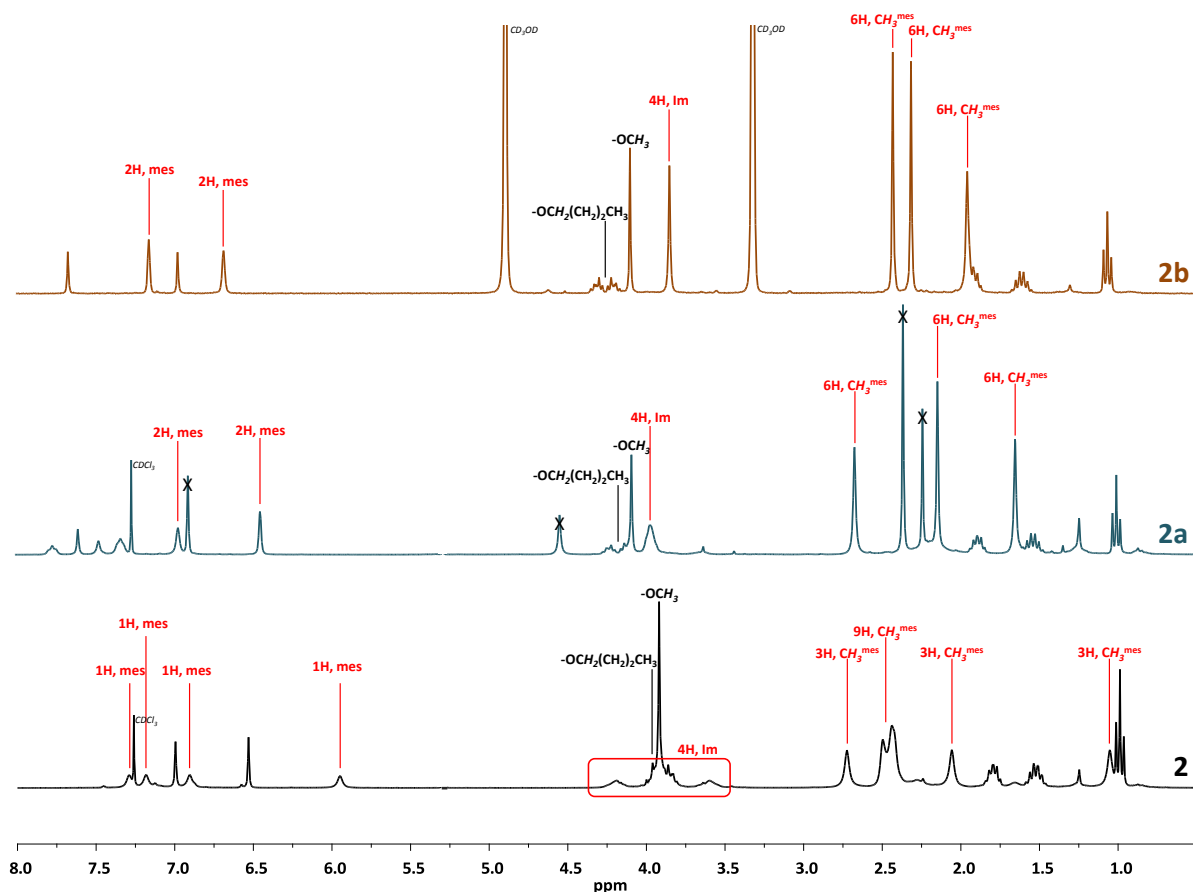


Figure 10. Comparison of the H_2IMes proton resonances (300.36 MHz) in the complexes **2**, **2a** ($CDCl_3$) and **2b** (methanol- d_4), (crossed out peaks in **2a** originate from free H_2IMes molecules)

While the 6 methyl groups of the mesityl moieties split into 5 peaks in the neutral complex (**2**), the signals are reduced to 3 (6 magnetically equal protons each) in the cationic complexes (**2a** and **2b**). Four identical protons of the saturated imidazole ring appear as one resonance in **2a** and **2b** instead of one broad multiplet in the neutral complex **2**. Compared to the pyridine adduct **2a**, the singlet (4H, Im) in **2b** is sharpened and slightly shifted to lower ppm values.

Furthermore, the 4 aromatic protons of the mesityl moiety occur as 2 sharp singlets in the cationic species, whereas in the spectrum of the neutral complex 4 broad singlets were found.

3.2.3 X-ray Structures

For stereochemical analysis and further characterization, crystals were grown by slowly evaporating a solution of the purified complexes **1-4** in CH₂Cl₂ (not until dryness) and measured by single crystal X-ray diffraction. Molecular structures have been obtained from the benzyloxy (**1**) and hexyloxy (**3**) derivatives (see Figures 11 and 12). Measurement of complex **2** was not feasible due to drying of the crystals and complex **4** did not crystallize. Complex **3** is representative for the molecular geometry of **2** and **4** due to characteristic ¹H NMR shifts, especially in the carbene region (18.44-18.50 ppm).

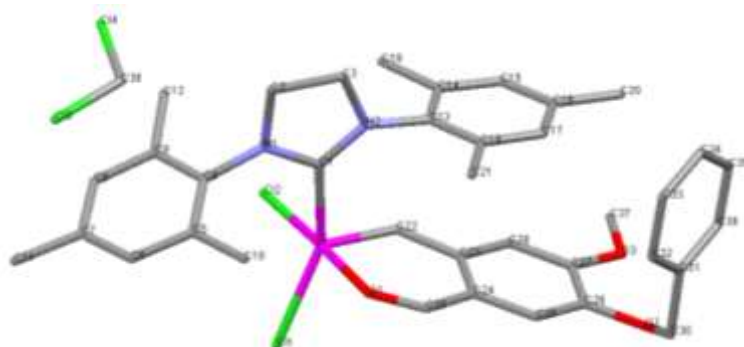


Figure 11. Molecular structure of complex **1**·CH₂Cl₂ (hydrogen atoms are hidden due to better clarity)

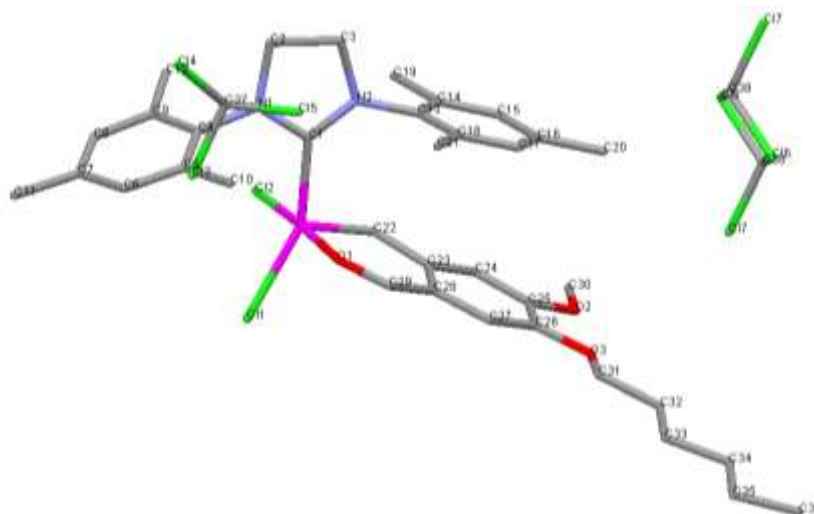


Figure 12. Molecular structure of complex **3**·(CDCl₃)₃ (hydrogen atoms are hidden due to better clarity)

As assumed, these complexes bear all the typical *cis*-dichloro geometry. The coordination geometry around the ruthenium is square pyramidal, whereas the base is formed by the carbonyl oxygen O(1), the C(1) atom of the H₂IMes ligand and the two chloro ligands Cl(1) and Cl(2). The carbene carbon C(22) occupies the apical position.

The molecular structures in Figures 11 and 12 reveal a parallel arrangement of the *N*-mesityl moieties and the chelating 2-formylbenzylidene ligand (π -stacking effect).⁹

In order to determine the influence of the different substituents located on the chelating carbene ligand in complexes **1** and **3**, corresponding bond lengths of the metallacycle, the anionic ligands and the NHC-ligand have been compared to each other as well as to reference complex **A** (Figure 13).

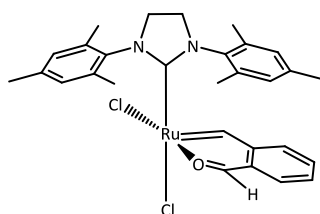


Figure 13. Complex **A** (*cis*-dichloro(2-formylbenzylidene- κ^2 (C,O))(1,3-bis(2,4,6-trimethylphenyl)-4,5-dihydroimidazol-2-ylidene)ruthenium(II))

Table 4. Selected bond lengths of complexes **1**, **3** and **A**²⁰ (Å)

	complex 1		complex 3		complex A
Ru-C(22)	1.830(1)	Ru-C(22)	1.832(5)	Ru-C(41)	1.827(2)
Ru-C(1)	2.013(1)	Ru-C(1)	2.007(5)	Ru-C(11)	2.004(2)
Ru-O(1)	2.0583(9)	Ru-O(1)	2.049(3)	Ru-O(49)	2.0487(16)
Ru-Cl(1)	2.3877(3)	Ru-Cl(1)	2.377(2)	Ru-Cl(2)	2.3600(6)
Ru-Cl(2)	2.3654(3)	Ru-Cl(2)	2.365(1)	Ru-Cl(1)	2.3548(6)
C(22)-C(23)	1.454(2)	C(22)-C(23)	1.453(7)	C(41)-C(42)	1.458(3)
C(23)-C(24)	1.414(2)	C(23)-C(28)	1.419(7)	C(42)-C(47)	1.420(3)
C(24)-C(29)	1.436(2)	C(28)-C(29)	1.433(7)	C(47)-C(48)	1.445(3)
C(29)-O(1)	1.248(2)	C(29)-O(1)	1.251(6)	C(48)-O(49)	1.242(3)

Compared to complex **A** the Ru-O(1) and both Ru-Cl bonds of complexes **1** and **3** are slightly elongated whereas the residual bond lengths of the metallacycle are marginal shortened.

²⁰ C. Slugovc, B. Perner, F. Stelzer, K. Mereiter, *Acta Cryst.* **2010**, *E66*, m154-m155

This little alteration is most likely a consequence of the electron donating substituents (OR residues) of the chelating carbene ligand. The stabilizing effect of these moieties leads to an elongation of the Ru-Cl bonds.

Table 5. Selected bond angles of complexes **1**, **3** and **A** (°)

complex 1		complex 3		complex A	
C(22)-Ru-C(1)	97.56(5)	C(22)-Ru-C(1)	97.8(2)	C(41)-Ru-C(11)	97.98(9)
C(22)-Ru-O(1)	91.13(5)	C(22)-Ru-O(1)	91.8(2)	C(41)-Ru-O(49)	91.12(8)
O(1)-Ru-Cl(1)	87.73(3)	O(1)-Ru-Cl(1)	86.7(1)	O(49)-Ru-Cl(2)	87.66(5)
C(22)-Ru-Cl(2)	90.32(4)	C(22)-Ru-Cl(2)	88.9(2)	C(41)-Ru-Cl(1)	89.81(7)
C(22)-Ru-Cl(1)	111.35(4)	C(22)-Ru-Cl(1)	109.6(2)	C(41)-Ru-Cl(2)	111.76(7)
Cl(1)-Ru-Cl(2)	90.31(1)	Cl(1)-Ru-Cl(2)	90.30(5)	Cl(2)-Ru-Cl(1)	89.76(2)
C(22)-C(23)-C(24)	123.5(1)	C(22)-C(23)-C(28)	123.0(5)	C(41)-C(42)-C(47)	123.7(2)
C(23)-C(24)-C(29)	122.5(1)	C(23)-C(28)-C(29)	122.8(5)	C(42)-C(47)-C(48)	122.0(2)
O(1)-C(29)-C(24)	125.8(1)	O(1)-C(29)-C(28)	126.2(5)	O(49)-C(48)-C(47)	125.4(2)
Ru-O(1)-C(29)	127.88(9)	Ru-O(1)-C(29)	126.7(3)	Ru-O(49)-C(48)	128.47(1)

Overall, the bond angles are very similar in all three complexes and no considerable deviations are observed. Obviously, the conducted ligand modifications are of minor steric importance and do not have implications on the geometry of the final complexes.

3.2.4 Solubility

For the novel complexes **1-4**, the design was construed in a manner to obtain an initiator soluble in nonpolar solvents. In order to assess the solubility of the synthesized complexes in varying solvents, solubility tests were performed. Therefore, 1 mg of the respective complex was dissolved in CH₂Cl₂ and stirred in a vial until complete drying of the solvent. This pretreatment was necessary to gain a uniform crystallite size for comparability.

The tests were performed by adding 1 mL of the required solvent (CH₂Cl₂, Cy, Et₂O, MeOH, DCPD) and stirring at room temperature (33°C for DCPD). The results were determined by optical inspection and classification into groups according to the solubility of the initiator after 20 minutes of stirring (Table 6).

- completely dissolved, immediately (clear green solution)
- partially dissolved, solid particles remaining (slightly cloudy green solution)
- hardly dissolved, majority of the complex only dispersed (cloudy green solution)
- dispersed, not dissolved (greenish dispersion)

Table 6. Results of the solubility test

complex	1	2	3	4	A
CH ₂ Cl ₂	●	●	●	●	●
Cy	●	●	●	●	●
Et ₂ O	●	●	●	●	●
MeOH	●	●	●	●	●
DCPD	●	●	●	●	●

The presented solubilities in these solvents are given at a concentration of 1 mg/mL (0.001 mol/L). In polymerization processes the applied amount of initiator is usually much lower, so this is an acceptable simulation of polymerization conditions.

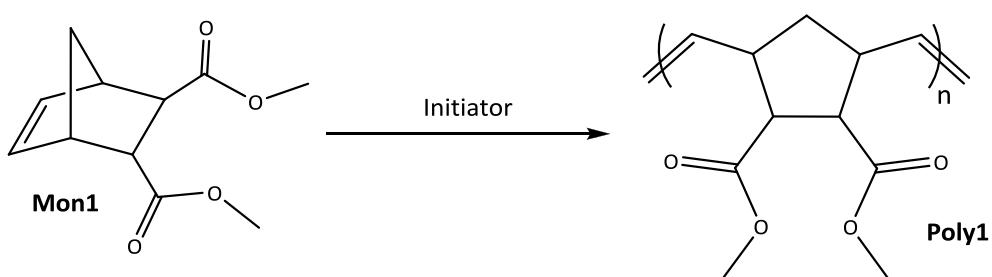
A significant improvement of the solubility in apolar solvents was only detected for complex **4** (octyloxy moiety), which is at least slightly soluble in all of the selected solvents.

Complex **1** showed in general a very poor solubility, even in CH₂Cl₂. A possible explanation for this bad solubility behaviour could be the favoured crystallization due to the benzyloxy residue.

3.2.5 Ring Opening Metathesis Polymerization (ROMP)

To assess the catalytic activity of the prepared complexes, ring opening metathesis polymerization (ROMP)¹⁵ of norbornene derivatives (methyl ester (**Mon1**) and DCPD (**Mon2**)) was performed under standard conditions. In order to compare the catalytic performance in ROMP, complex **A** (unsubstituted aldehyde type, see Figure 13) was used as reference.

3.2.5.1 ROMP of **Mon1**



Scheme 7. Polymerization procedure of *endo/exo*-dimethyl-bicyclo[2.2.1]hept-5-ene-2,3-dicarboxylate (**Mon1**)

In order to achieve more information about the initiation/propagation processes, reactions were carried out in NMR tubes at room temperature and spectra were recorded every 12 to 24 h (M:I = 10, for experimental details see section 5.2.5.2).

The time/conversion plots of polymerizations with initiators **1-4** (see Figure 14) indicate a very latent behavior at room temperature for all complexes with poor initiation as well as slow propagation (see also results of the standard polymerization procedure, Table 7). After 7 days, initiators **2, 3, 4** and **A** reached the maximal conversion (approx. 95 %). Complex **1** reached only 60 % after 14 days, most probably due to the poor solubility in CDCl_3 . The most striking difference concerning the conversion appears after 3 days. Whereas initiators **2, 3** and **4** reach a conversion of 84 %, **1** only reaches 24 %.

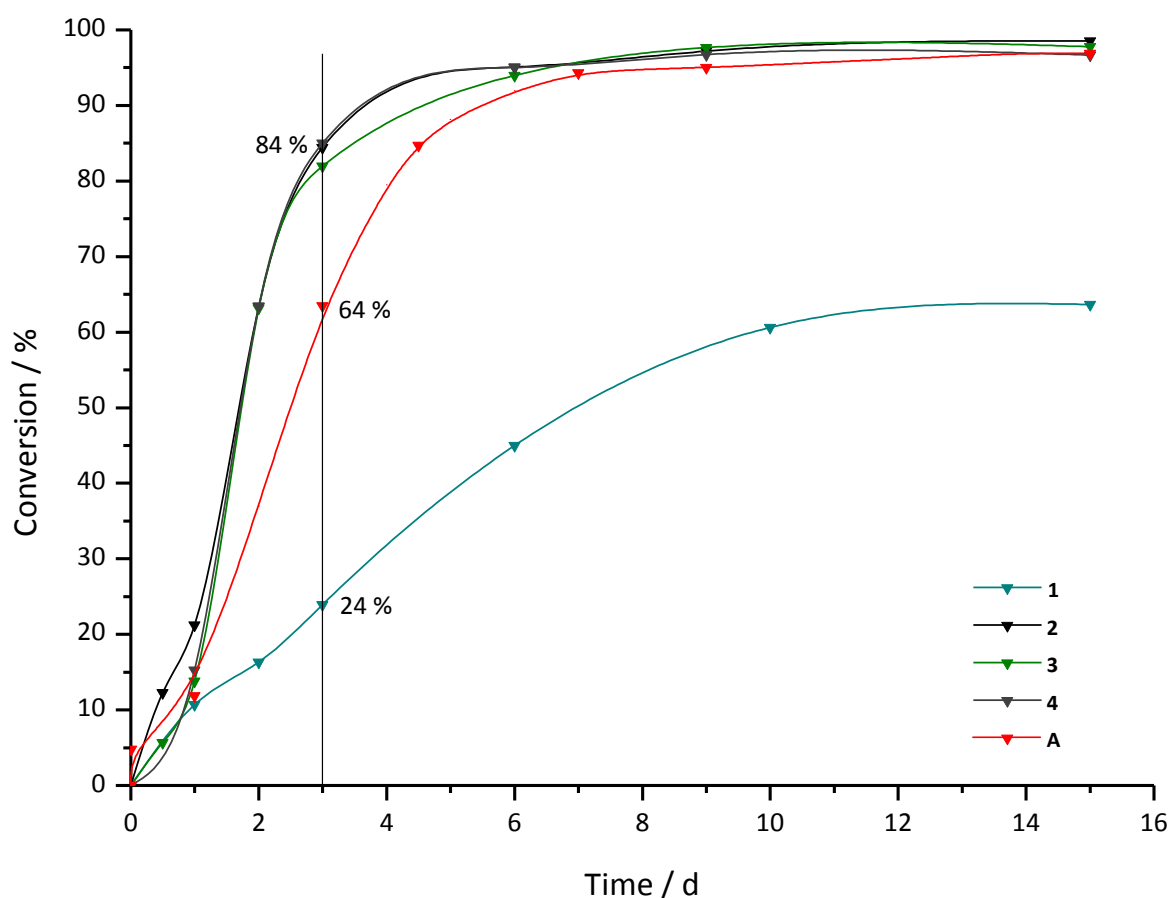


Figure 14. Time/conversion plot of polymerizations in NMR tube

A closer look at the recorded ^1H NMR spectra before and during the polymerization showed an additional carbene proton resonance at 19.20 ppm (accounting for approximately 10 %) for complexes **2, 3** and **4**, but not for **1**. As this peak is disappearing with ongoing polymerization, a correlation with the initiation is obvious (Figure 15). Differences in conversion are subsequently associated with this carbene species at about 19.20 ppm.

However, an interesting fact is that an analogue carbene species is not observed in the spectra of **A**. Nevertheless, **A** is clearly more active than complex **1**, which can be explained by very poor solubility of **1** in contrast to complex **A**. In solution, an isomerization process is much more likely, and thus **A** possibly forms the respective carbene species *in situ* before initiating the polymerization. In case of **2**, **3** and **4**, the second (and obviously most active) species is already present in larger amounts from the very beginning, which leads to the fastest conversion within this series. Even if this important second carbene species was not observed in the polymerization series with complex **1**, the same activating rearrangement is substantiated upon ^1H NMR measurements in methanol, where **1** is better soluble and a resonance at 19.22 ppm appeared (compare section 5.2.4.1). Figure 15 displays the carbene region of complex **2** in the course of the polymerization.

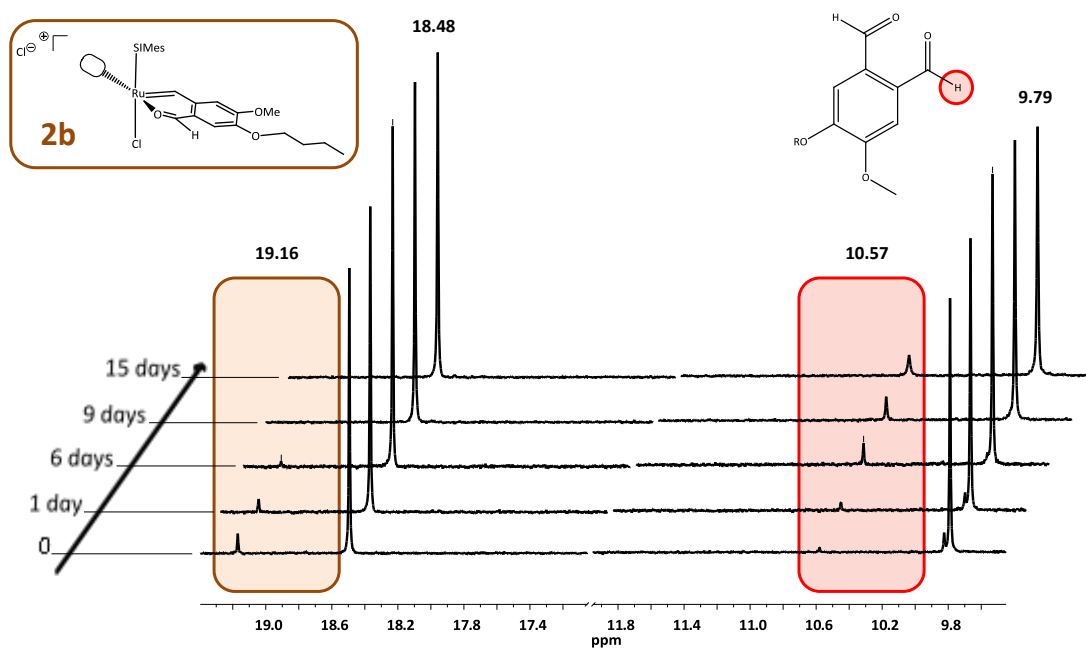


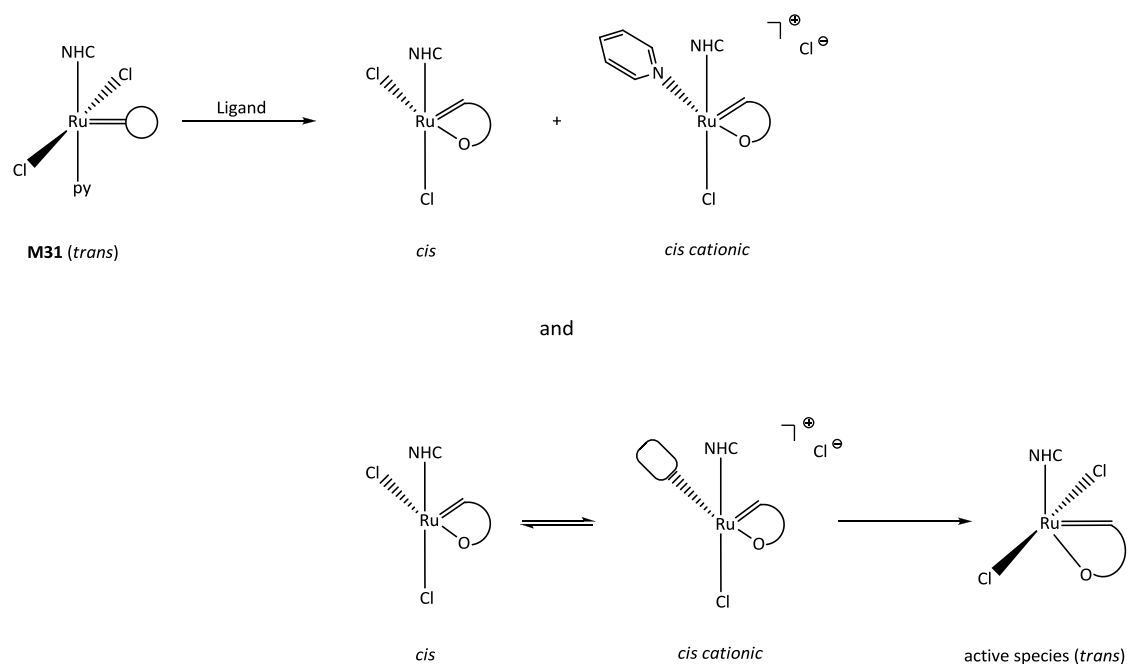
Figure 15. Carbene and aldehyde proton resonances during the ROM polymerization progress of **Mon1** with initiator **2** and assumed decomposition compound (300 MHz, CDCl_3)

Obviously, the carbene resonance at 19.20 ppm represents the active species or an intermediate on the way to the active species respectively, because it disappears during ongoing polymerization whereas the main carbene species (neutral *cis*-dichloro structure) is not consumed. Concurrently a peak at 10.57 ppm appears which is considered to be a decomposition product of the cationic complex **2b** (Figure 15). This is another argument for

this species to be the (*pre*-)active species. A faster decomposition implies a more labile complex and thus a more active system.

As already mentioned in chapter 3.2.2, it is most likely that in methanol a rearrangement to complex **2b** takes place. In order to test if methanol is a possible trigger for this system, the polymerization was carried out in the presence of 10 mol% methanol. Unfortunately the expected effect did not occur. Thus the polymerization progress was equally compared to the one in the absence of methanol. Obviously such a small amount of methanol is not enough to force a complete rearrangement of the neutral *cis*-dichloro conformation into the (*pre*-)active cationic species. Unfortunately a polymerization carried out in methanol as solvent is not feasible due to the insolubility of **Poly1**.

To explain the mechanism to the catalytically active species further experiments and investigations have to be accomplished. If the pathway to the active species is resolved, the polymerization using these initiators can be optimized. In Scheme 8 a possible pathway to the active species, recently disclosed in our group¹⁹, is shown.



Scheme 8. Possible pathway to the active species

The synthesis of ruthenium complexes starting from **M31** yields the neutral *cis*-dichloro complex and the cationic pyridine complex, in a ratio of 4:1. After separation of these two species, a third species, which is considered to be the (*pre*-)active complex occurred. Due to this retarded formation of the third complex, the question whether this species is accessible only via the neutral *cis* complex or also via the cationic pyridine adduct arose. Also the fact, whether this complex is the active species itself, or if it is just another intermediate during the formation of the active species remains unclear.

ROM polymerizations of **Mon1** were also carried out following a standard procedure using a M:I ratio of 300 at a monomer concentration of 1 mol/L. Reactions were performed under inert conditions at RT and 40°C in dichloromethane and at 80°C in toluene. The obtained polymers were analyzed by gel permeation chromatography (GPC) to determine the average molecular weight (M_n , number molar mass), which will allow an indirect comparison of initiation rate to propagation rate constants (k_i/k_p) (1). The results of this polymerization series are listed in Table 7 (weight molar mass M_w , polydispersity index *PDI*).

$$MWD \approx k_p/k_i \quad (1)$$

Table 7. Reaction conditions and GPC results of **Poly1**

Poly1	initiator	solvent	T / °C	reaction time	Yield	M _n / g·mol ⁻¹	PDI
A_1	A	CH ₂ Cl ₂	RT	17 d	-*	445700	2.1
1_1	1	CH ₂ Cl ₂	RT	17 d	-*	<i>n.d.</i>	<i>n.d.</i>
2_1	2	CH ₂ Cl ₂	RT	10 d	92 %	592400	1.8
3_1	3	CH ₂ Cl ₂	RT	10 d	92 %	589800	1.7
4_1	4	CH ₂ Cl ₂	RT	10 d	97 %	559000	1.8
A_2	A	CH ₂ Cl ₂	40	1 d	73 %	702600	2.0
1_2	1	CH ₂ Cl ₂	40	1 d	74 %	621600	1.9
2_2	2	CH ₂ Cl ₂	40	2 d	96 %	859400	1.9
3_2	3	CH ₂ Cl ₂	40	2 d	96 %	626800	1.7
4_2	4	CH ₂ Cl ₂	40	2 d	94 %	835100	1.7
A_3	A	toluene	80	0.5 h	80 %	91200	2.2
1_3	1	toluene	80	3 h	71 %	92800	2.3
2_3	2	toluene	80	1 h	93 %	82500	2.3
3_3	3	toluene	80	1 h	90%	104500	2.0
4_3	4	toluene	80	1 h	96%	65700	2.6

n.d. = not determined

*not observed due to frequent NMR sampling

Polymerizations with initiator **1** at room temperature were not reproducible regarding reaction times and achieved polymer weight distribution, which is supposedly due to the extremely low activity. Results are therefore not included herein.

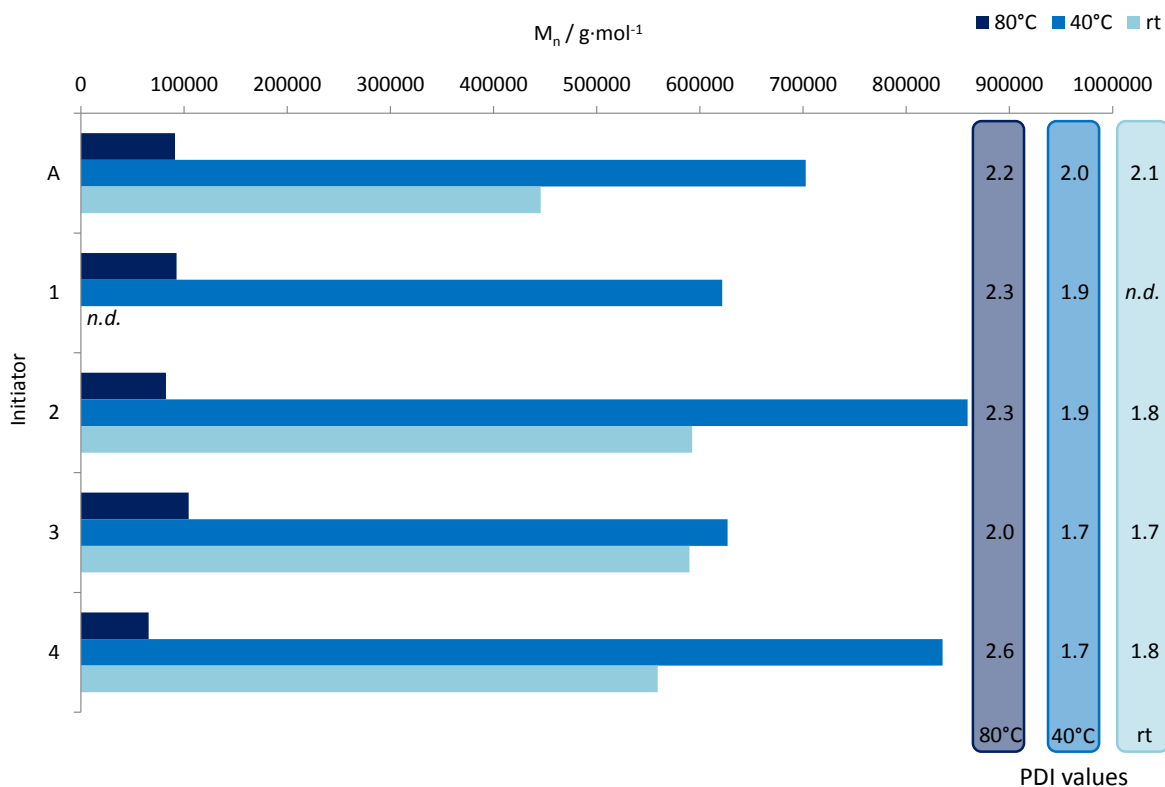


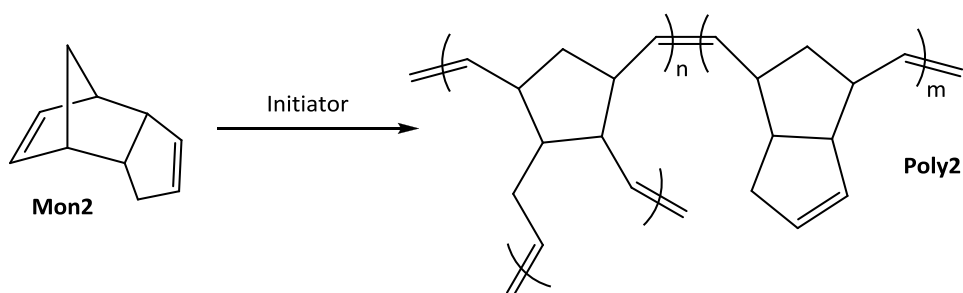
Figure 16. Comparison of the GPC results of **Poly1**, catalyzed with **A**, and **1-4** at different conditions

Figure 16 discloses the varying results of **Poly1** synthesized with the latent cis-dichloro ruthenium complexes **A** and **1-4** at different polymerization conditions. These initiators lead to remarkably high M_n values, resulting from high propagation compared to the initiation (k_i/k_p is distinctly less than 1). Within this series the propagating species is considered to be equal for all initiators, which allows a direct correlation of the determined M_n values to k_i . An impact of the different alkoxy residues is not recognizable at this point.

The polymerization at 80°C in toluene yields **Poly1** with comparably low M_n values, but high polydispersity indices (PDI). This indicates an explicitly higher initiation rate constant (k_i) in opposition to the obtained values from the polymerizations at 40°C and room temperature. Interestingly the M_n values from **Poly1** synthesized at 40°C are significantly higher than the M_n values from the series at RT, whereas PDI values are in the same range.

3.2.5.2 ROMP of **Mon2**

Bulk ROM polymerizations of dicyclopentadiene (DCPD, Scheme 9) were performed at RT and at 60°C in an oven. The required amount of initiator (loadings 40, 20, 10, 6.6, 5 and 3.3 ppm) was extracted from a stock solution, topped up to an adding volume of 300 μL and injected into 5 mL of DCPD. The polymerization progress was monitored by tipping into the tube with a spatula and noting the viscosity based on a self-developed scale reaching from 0 to 100 (Table 8). Experimental details are mentioned in chapter 5.2.5.3.



Scheme 9. ROMP of Dicyclopentadiene (**Mon2**)

Table 8. Scale to estimate the viscosity and hence the polymerization progress

Category	Specification
0	no reaction, mixing possible
5	slightly viscous
10	viscous
15	more viscous
20	highly viscous
25	stacked, highly viscous (sticky)
30	gelation, supple (sticky)
35	solid, gel-like (slightly sticky)
40	solid, gel-like (hardly sticky)
50	solid, very elastic, soft
60	solid, rather elastic
70	solid, elastic
80	solid, few elastic
90	solid, hardly elastic
95	solid, barely cured
100	solid, fully cured (brittle)

Figures 17 and 18 show the polymerization progress of **Mon2** using the synthesized initiators and reference compound **A** at room temperature and at 60°C. Compared to **A**, the four modified complexes show a more latent behavior, especially at room temperature.

Again, as shown in the polymerization of **Mon1**, initiator **1** exhibits the lowest conversion. Complexes **2**, **3** and **4** show a modest conversion within the first 48 hours, whereas the conversion rises with increasing chain length of the residues (butyloxy (**2**), hexyloxy (**3**) and octyloxy (**4**)). This can be explained by the better solubility of the complexes and hence a better polymerization performance.

The moderate conversions at room temperature indicate a latent behaviour of the initiators, but not a complete latency. In case of total latency no conversion should proceed. However, the polymerization carried out at 60°C proceeded more satisfyingly. At least initiators **3** and **4** reached full conversion within the first hour, which complies quite well with reference compound **A**. Complexes **1** and **2** show a similar polymerization progress, but reach again only moderate conversions. Therefore the decisive improvement according solubility lies between the introduced butyloxy and hexyloxy residue.

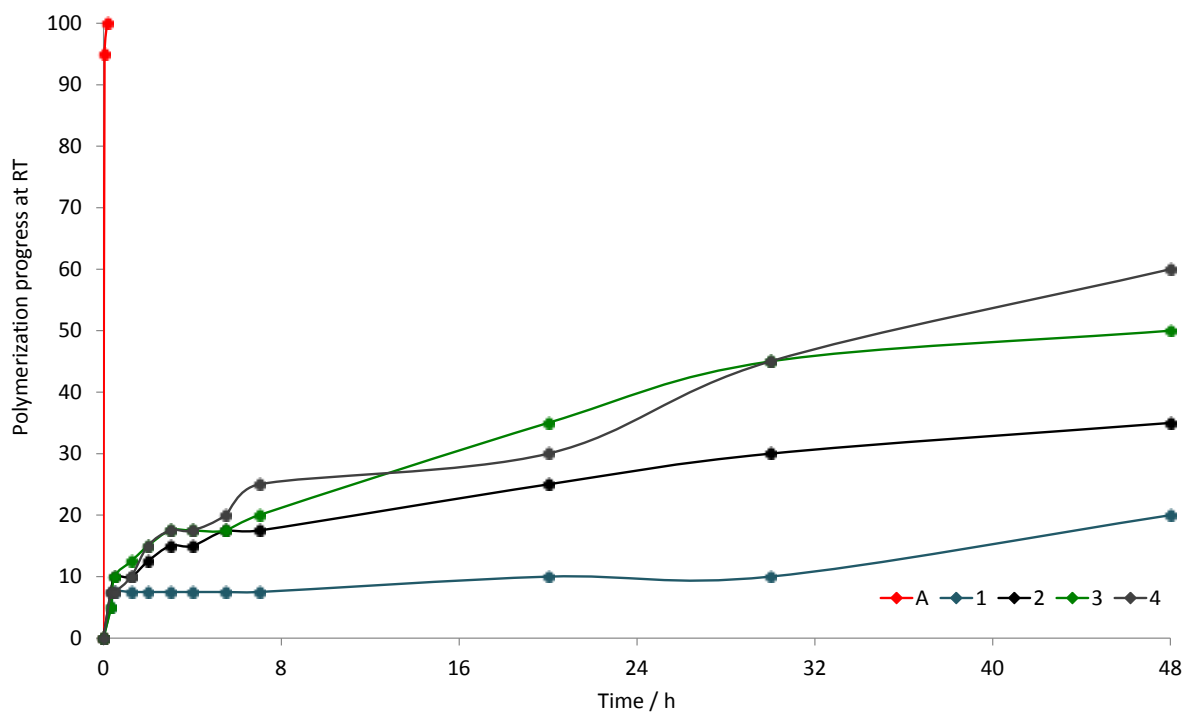


Figure 17. Polymerization progress of monomer 2 at RT (initiator loading = 40 ppm)

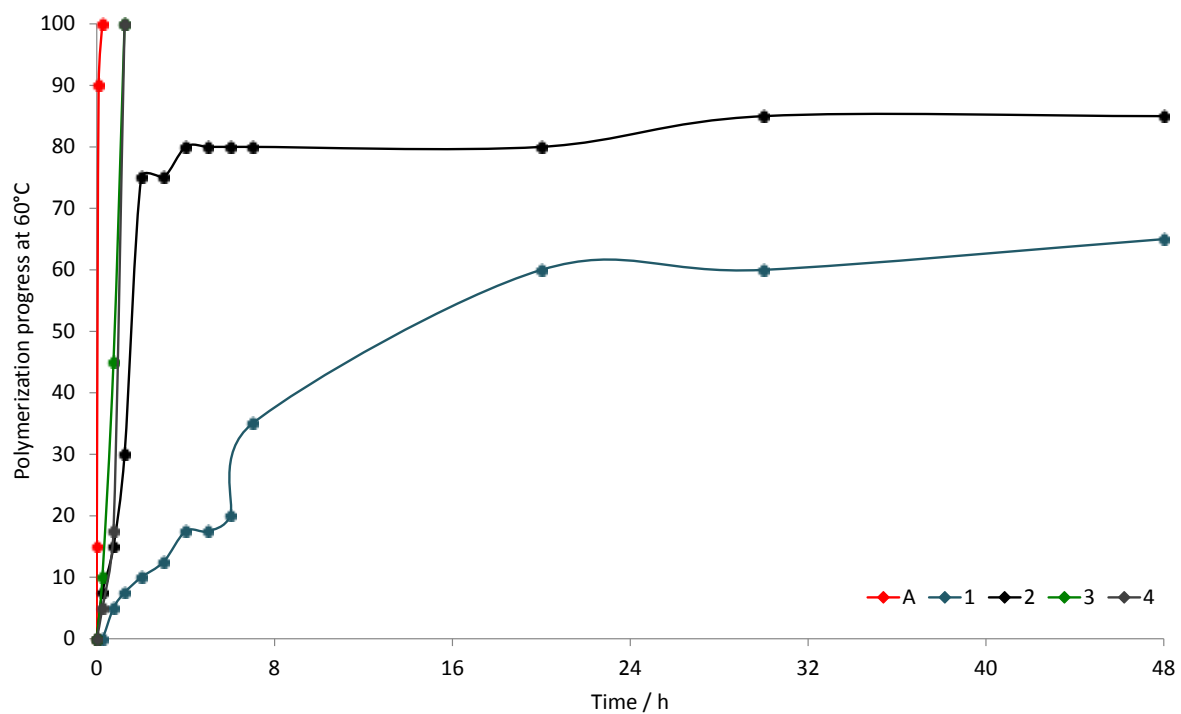


Figure 18. Polymerization progress of monomer 2 at 60°C (initiator loading = 40 ppm)

A difficulty performing these tests arose in the not given reproducibility of initiator **1**, especially at room temperature (see Figure 19). The irregularity is clearly evident as the sample with an initiator loading of 6.6 ppm showed the highest and the one with 40 ppm initiator the lowest conversion.

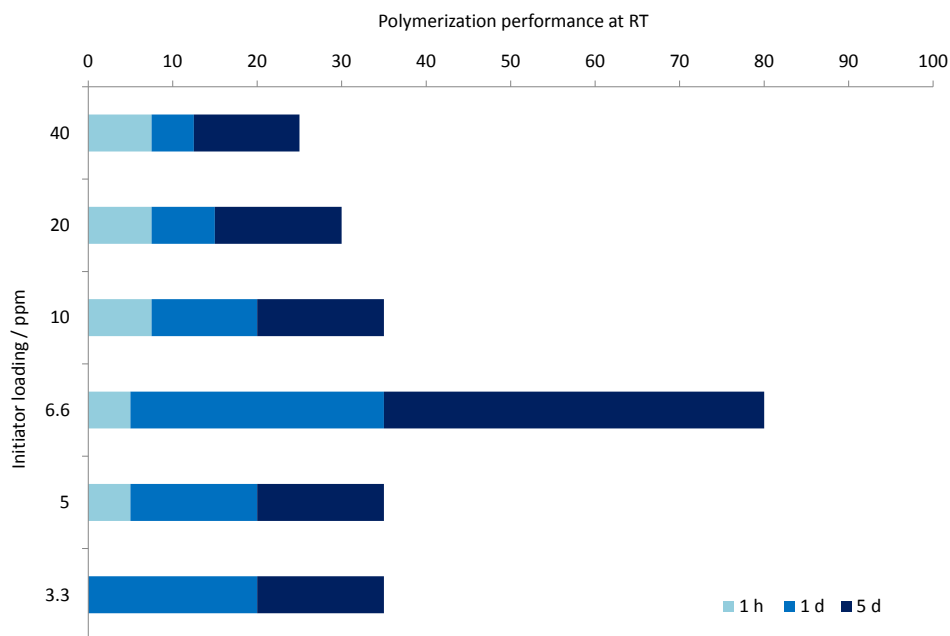


Figure 19. Polymerization performance of initiator **1** at RT (comparison of all loadings)

Figures 20 and 21 show the polymerization performance of the title compounds compared to **A** at room temperature and 60°C. These staggered diagrams clearly illustrate once more the reached conversion within 48 hours. Especially at room temperature the latent behavior of initiators **1-4** is explicitly visible.

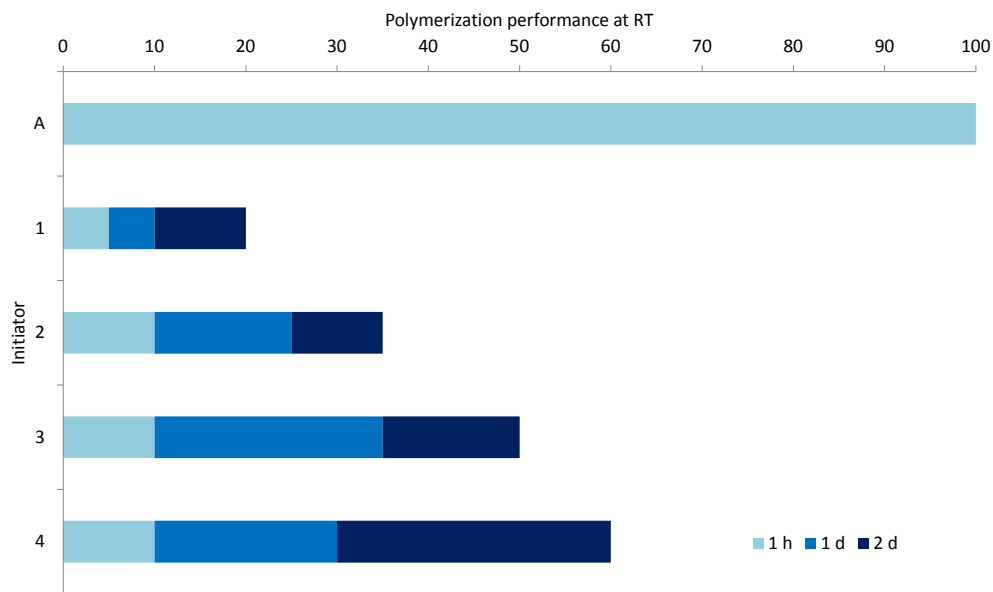


Figure 20. Comparison of the polymerization performance at RT (loading = 40 ppm)

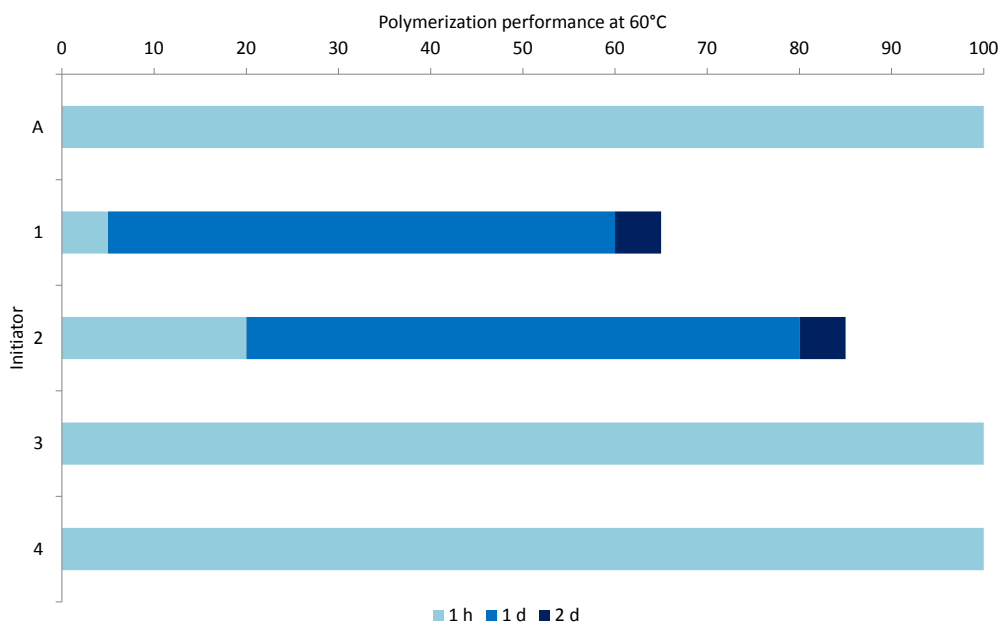


Figure 21. Comparison of the polymerization performance at 60°C (loading = 40 ppm)

3.2.5.3 Simultaneous Thermal Analysis (STA)

STA is the simultaneous application of thermogravimetry (TGA) and differential scanning calorimetry (DSC) of one sample in one single instrument. The weight changes of the sample are measured as a function of temperature (or time) under a controlled atmosphere. This method turned out to be a useful tool to detect the switching temperature of initiators. Therefore a thermally triggered bulk polymerization of DCPD (**Mon2**) in simultaneous thermal analysis was performed.¹⁶

STA samples were prepared by mixing 1 mL of DCPD with a solution of the required amount of initiator (40 ppm, extracted from a stock solution) topped up to 60 μ L. Due to the very latent behaviour of the initiators at room temperature a shock freezing in liquid nitrogen of the samples was not necessary. About 13 mg were transferred into a DSC pan which was immediately subjected to the STA run.

While the polymerization progress at room temperature proceeds very slowly and incompletely, it can be controlled and improved by performing the reaction at the optimal temperature. To enhance the polymerization performance and the reached conversion, simultaneous thermal analysis was used to detect the triggering temperature of the initiators.

Figure 22 shows a representative plot of the simultaneous thermal measurement with complex **2**. The results for the other complexes are listed in Table 9. The polymerization curve in all DSC diagrams show two peaks. The first peak value represents the ROMP of DCPD and the second one originates from the cross linkage. These two peaks usually fall together when the initiation rate is sufficiently high to provide enough exothermic energy for both processes.²¹ The relatively high mass loss compared to **A** is caused by the high *onset* temperature of the initiators. Before polymerization starts, a part of the DCPD decomposes due to Retro-Diels-Alder reaction, yielding volatile cyclopentadiene. As can be seen in Table 9, all temperature ranges for the polymerization are comparable. An irregularity occurs regarding the mass loss and *onset* temperature with initiator **2**. The satisfying *onset* temperature (62.9°C) does not explain the high mass loss of 33 %. Most likely this was caused by weighing errors or other operating problems.

²¹ M. R. Kesser, G. E. Larin, N. Bernklau, *J. Therm. Anal. Cal.* **2006**, *85*, 7-12

Interesting are the peak values in correlation with the *onset* temperatures. Initiators **1** and **2** have the lowest *onset* temperatures but the highest peak values. This indicates a slow propagation and could also be an explanation for the quite high mass loss.

The obtained results from the simultaneous thermal analysis agree with the results of the ROMP of DCPD at room temperature and 60°C (compare section 3.2.5.2).

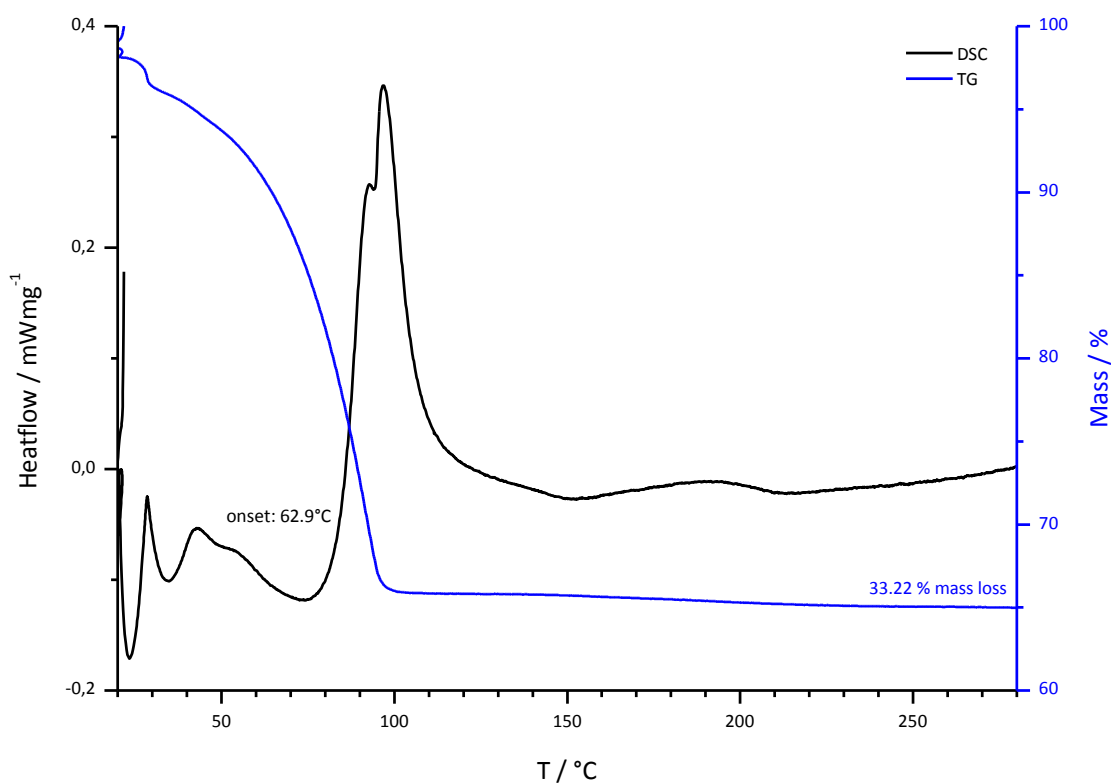


Figure 22. DSC and TGA diagrams for ROMP of DCPD with initiator **2** (40 ppm, heating rate 3°C/min)

Table 9. Results of STA for Initiators **1-4** and **A** (reference)

Initiator	1	2	3	4	A
Heat of reaction / J·g ⁻¹	190	133	222	144	131
Peak / °C	91	97	82	88	72
Onset / °C	80	63	70	80	24
Offset / °C	105	106	82	100	86
T-range / °C	19	18	27	16	23
Heat flow / mW·mg ⁻¹	0.527	0.410	0.465	0.485	0.317
Mass loss / %	23	33	20	30	10

The simultaneous thermal analysis provided a detailed illustration of the catalytic activity in ROMP of DPCD. The received results show that initiators **1** and **2** would be the first choice concerning the *onset* temperature, but the propagation is too slow. Looking at the peak value and the *offset* temperature of complexes **3** and **4**, they would be suitable for DCPD, but the *onset* temperature is too high which causes the substantial mass loss. The most promising initiator of this series for DCPD is complex **3** due to its comparable low peak value (82.4°C), the small difference between *onset* and *offset* temperatures and the low mass loss.

4 Conclusion and Outlook

This work discloses the synthesis and characterization of novel latent *cis*-dichloro ruthenium complexes bearing an aldehyde functionality as the chelating carbene moiety. The initiators were designed in a manner to increase the solubility of these compounds in DCPD to establish a new catalyst system for this promising monomer.

The synthesis and characterization was successful, and also two cationic side products were described. The application in ROMP of **Mon1** and **Mon2** proceeded moderately and showed a very latent behaviour of initiators **1-4**. It has to be noted, that results obtained from bulk polymerization of DCPD must not directly be compared to polymerization of **Mon1** that were carried out in solution. Most important, the solubility of the initiator in the respective reaction set up has to be carefully evaluated. To improve the polymerization properties, the mechanism of the rearrangement to the catalytically active species has to be found and experimentally proven. With this knowledge, a triggering system besides the incomplete thermal triggering for these initiators, e.g. activation with methanol could be developed.

The introduction of different alkoxy residues in the chelating ligand led to improved solubility of the complexes in neat DPCD maintaining a growing effect with increasing chain length. This trend is also valid for the performance in bulk ROM polymerization of DCPD (**Mon2**) within this complex series. However, the different residues did not affect the solution polymerization of **Mon1**.

Besides the application in the bulk ROM polymerization of DCPD, a utilization of the synthesized initiators in the polyHIPE* system^{22,23} and thus replacing of commercial initiators is possible. Therefore, a precise switchability, a high initiation rate as well as fast propagation of the *pre*-catalysts are required. The high demands of this system are caused by the thermodynamical instability of the emulsion. Initiators **3** and **4** have been tested in the polyHIPE system, but turned out to be too latent.

* HIPE = high internal phase emulsion

²² S. Kovačič, K. Jeřábek, P. Krajnc and C. Slugovc, *Polym. Chem.*, **2011**, xx, 1-5 (DOI: 10.1039/c2py00518b)

²³ S. Kovačič, K. Jeřábek, P. Krajnc and C. Slugovc, in progress

Summarizing, four novel ruthenium complexes and an approach for modifying the solubility of these compounds have been disclosed. Further work on this topic will include the development of switchability of the system by resolving the mechanism. Additionally, investigations to further increase the solubility of the complexes in DCPD have to be accomplished.

5 Experimental

5.1 Instruments and Materials

All chemicals for the synthesis of ligands were purchased from commercial sources (Sigma Aldrich, Fluka or Alfa Aesar) and used without further purification. Complex **M31** ([1,3-bis(2,4,6-trimethylphenyl)-2-imidazolidinylidene]dichloro(3-phenyl-1H-inden-1-ylidene)(pyridyl)ruthenium(II) for initiator synthesis was obtained from UMICORE AG & Co. KG. (H₂IMes)(2-formylbenzylidene-κ²(C,O))Cl₂Ru (**A**) as reference compound was available for use by Anita Leitgeb, TU Graz. Unless specified otherwise, solvents and auxiliary materials were used as purchased.

For TLC silica gel 60 F₂₅₄ on aluminium sheets (Merck) was used. Visualization was done by exposure with UV light and / or dipping into an aqueous solution of KMnO₄ (0.1 %).

Silica gel 60 (220-440 mesh ASTM) was used for column chromatography.

Polydispersity indices (PDI) and molecular weight data were determined by gel permeation chromatography (GPC) using THF as eluent. Device setup is composed of a Merck Hitachi L6000 pump (delivery volume: 1 mL/min), separation columns of Polymer Standards Service (5µm grade size) and a refractive index detector from Wyatt Technology. For calibration polystyrene standards from Polymer Standard Service were used.

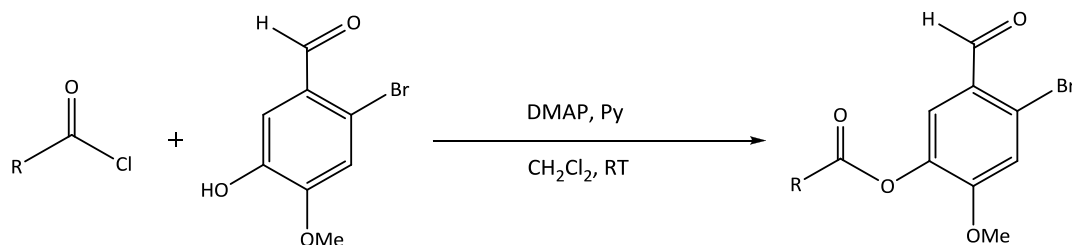
NMR spectroscopy (¹H, ¹³C) was done on a Bruker Avanze 300 MHz spectrometer and individual measurements were performed on a Varian INOVA 500 MHz spectrometer. Deuterated solvents were obtained from Cambridge Isotope Laboratories Inc. and remaining peaks were referenced according to literature.²⁴ Peak shapes are specified as follows: s (singlet), bs (broad singlet), d (doublet), dd (doublet of doublets), t (triplet), q (quadruplet), m (multiplet).

X-ray crystal structures were recorded on a Bruker Kappa APEX II diffractometer using Mo Kα radiation by Roland Fischer and Petra Wilfling, Institute for Inorganic Chemistry, Graz University of Technology.

²⁴ H.E. Gottlieb, A. Kotlyar, A. Nudelman, *J. Org. Chem.* **1997**, *62*, 7512

5.2 Syntheses

5.2.1 Esterifications

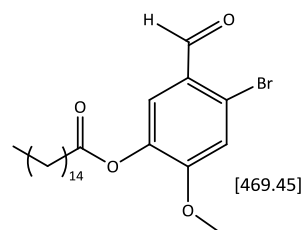


Scheme 10. Reaction scheme for the esterification of the hydroxy group¹⁸

5.2.1.1 4-Bromo-5-formyl-2-methoxyphenyl palmitate (**P5**)

Palmitic acid (500.1 mg, 1.95 mmol, 1.0 eq) was dissolved in thionyl chloride (2.0 mL, 27.4 mmol, 14 eq), heated to 80°C and stirred for 24 h with reflux cooling. Excessive thionyl chloride was removed through distillation. 2-bromo-5-hydroxy-4-methoxy benzaldehyde (450.5 mg, 1.95 mmol, 1.0 eq) was dissolved in degassed CH₂Cl₂ (15 mL), pyridine (0.41 mL, 5.07 mmol, 2.6 eq) and 4-dimethylaminopyridine (11.9 mg, 0.10 mmol, 0.05 eq) were added. This solution was dropped carefully (HCl formation) to the remaining palmitic acid chloride (brown oil) and stirred at room temperature for 48 h. The reaction mixture was extracted with aqueous HCl (5 %, 3 x 20 mL) and aqueous NaHCO₃ (saturated, 3 x 20 mL). The combined organic layer was dried with Na₂SO₄, filtered, evaporated and dried in vacuo, whereby white crystals appeared in the remaining brown oil. The crude product was purified by column chromatography (Cy/EtOAc, 10:1, (v:v), by sampling the spot at R_f = 0.51 (Cy/EtOAc, 5:1, (v:v))). Yield: 366.6 mg (40 %) white-brownish solid.

TLC: R_f = 0.51 (Cy/EtOAc, 5:1, (v:v))

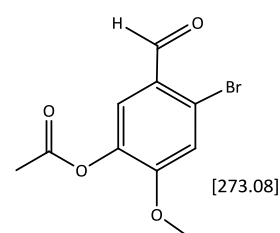


¹H-NMR: (δ, 20°C, CDCl₃, 300.36 MHz): 10.18 (s, 1H, CHO), 7.61 (s, 1H, ph⁶), 7.16 (s, 1H, ph³), 3.90 (s, 3H, OCH₃), 2.57 (t, 2H, ³J_{HH} = 7.5 Hz, COOCH₂(CH₂)₁₃CH₃), 1.74 (m, 2H, COOCH₂CH₂(CH₂)₁₂CH₃), 1.26 (bs, 24H, COO(CH₂)₂(CH₂)₁₂CH₃) 0.88 (t, 3H, ³J_{HH} = 6.6 Hz, COO(CH₂)₁₄CH₃)

5.2.1.2 4-Bromo-5-formyl-2-methoxyphenyl acetate (**P6**)

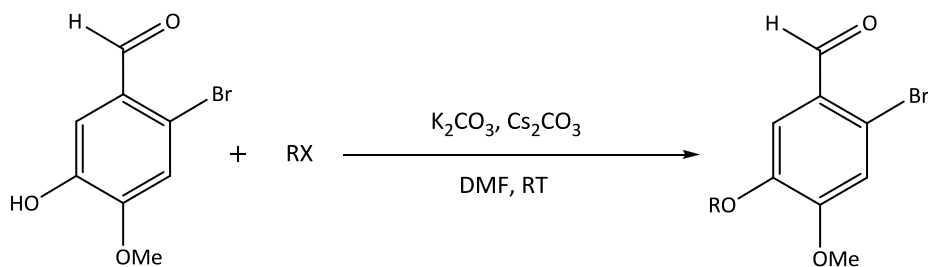
2-Bromo-5-hydroxy-4-methoxy benzaldehyde (200 mg, 0.87 mmol, 1.0 eq) was dissolved in degassed CH_2Cl_2 (5 mL), pyridine (182 μL , 2.25 mmol, 2.6 eq) and 4-dimethylaminopyridine (5.3 mg, 0.04 mmol, 0.05 eq) were added. Acetyl chloride (74 μL , 1.04 mmol, 1.2 eq) was added under ice cooling and the mixture was stirred for 24 h. Due to incomplete conversion, further acetyl chloride (37 μL , 0.52 mmol, 0.6 eq) was added. After another 24 h stirring, the solution was treated as described in the previous procedure. The remaining brown-white solid was purified by column chromatography (Cy/EtOAc, 10:1, (v:v), by sampling the spot at $R_f = 0.39$ (Cy/EtOAc, 5:1, (v:v))). Yield: 173.0 mg (73 %) white solid.

TLC: $R_f = 0.39$ (Cy/EtOAc, 5:1, (v:v))



$^1\text{H-NMR}$: (δ , 20°C, CDCl_3 , 300.36 MHz): 10.17 (s, 1H, CHO), 7.62 (s, 1H, ph^6), 7.17 (s, 1H, ph^3), 3.91 (s, 3H, OCH_3), 2.31 (s, 3H, COOCH_3)

5.2.2 Etherifications (5-Alkoxy-2-bromo-4-methoxy benzaldehydes)

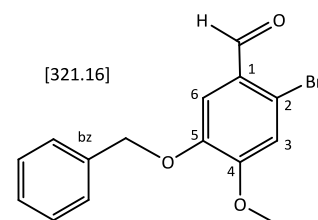


Scheme 11. Reaction scheme for the etherification of the hydroxy group¹⁶

5.2.2.1 5-Benzyloxy-2-bromo-4-methoxy benzaldehyde¹⁷

2-Bromo-5-hydroxy-4-methoxybenzaldehyde (500.0 mg, 2.16 mmol, 1.0 eq) was dissolved in acetone (10 mL) and K₂CO₃ (600.1 mg, 4.35 mmol, 2.0 eq) was added. Benzylbromide (257 μ L, 2.16 mmol, 1.0 eq) was added dropwise and the reaction mixture was stirred at room temperature. After 4 h the solution was filtered, evaporated and dried in vacuo. The remaining brown solid was purified by recrystallization from hot ethyl acetate. Yield: 375.4 mg (54 %) beige crystals.*

TLC: R_f = 0.37 (Cy/EtOAc, 5:1, (v:v))



¹H-NMR: (δ , 20°C, CDCl₃, 300.36 MHz): 10.16 (s, 1H, CHO), 7.48 (s, 1H, ph³), 7.47-7.28 (m, 5H, OCH₂(C₆H₅)), 7.07 (s, 1H, ph⁶), 5.16 (s, 2H, OCH₂(C₆H₅)), 3.95 (s, 3H, OCH₃)

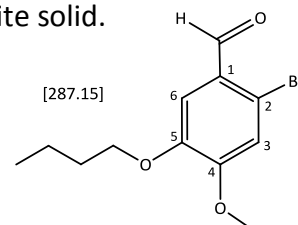
*Following preparations of this compound were also carried out in DMF by adding catalytic amounts of Cs₂CO₃ due to complete conversion and higher yields.

5.2.2.2 2-Bromo-5-butyloxy-4-methoxy benzaldehyde

K₂CO₃ (479.7 mg, 3.47 mmol, 2.0 eq), Cs₂CO₃ (28.3 mg, 0.09 mmol, 0.05 eq) and 1-iodobutane (279.0 μ L, 2.60 mmol, 1.5 eq) were added to a solution of 2-bromo-5-hydroxy-4-methoxybenzaldehyde (401.0 mg, 1.74 mmol, 1.0 eq) in DMF (15 mL). The reaction was

stirred for 17 h at room temperature. After complete conversion, the reaction mixture was quenched with H₂O deionized (20 mL) and extracted with Et₂O (2 x 25 mL). The combined organic layer was washed with aqueous NaOH (1 M, 2 x 20 mL) and aqueous NaCl (saturated, 2 x 20 mL). The organic layer was dried with Na₂SO₄, filtered, evaporated and dried in vacuo. The oily residue was purified by column chromatography (Cy/EtOAc, 10:1, (v:v), by sampling the spot at R_f = 0.54 (Cy/EtOAc, 5:1, (v:v))). Yield: 398.7 mg (80 %) white solid.

TLC: R_f = 0.54 (Cy/EtOAc, 5:1, (v:v))

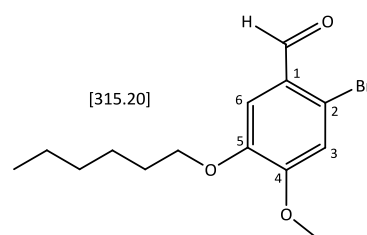


¹H-NMR: (δ, 20°C, CDCl₃, 300.36 MHz): 10.17 (s, 1H, CHO), 7.40 (s, 1H, ph³), 7.04 (s, 1H, ph⁶), 4.04 (t, 2H, ³J_{HH} = 6.8 Hz, OCH₂(CH₂)₂CH₃), 3.93 (s, 3H, OCH₃), 1.82 (m, 2H, OCH₂CH₂CH₂CH₃), 1.49 (m, 2H, O(CH₂)₂CH₂CH₃), 0.97 (t, 3H, ³J_{HH} = 7.4 Hz, O(CH₂)₃CH₃)

5.2.2.3 2-Bromo-5-hexyloxy-4-methoxy benzaldehyde

The preparation of 2-bromo-5-hexyloxy-4-methoxybenzaldehyde was performed as mentioned above. 2-Bromo-5-hydroxy-4-methoxybenzaldehyde (511.6 mg, 2.21 mmol, 1.0 eq), K₂CO₃ (612.0 mg, 4.43 mmol, 2.0 eq), Cs₂CO₃ (36.1 mg, 0.11 mmol, 0.05 eq) and 1-iodohexane (490.2 μL, 3.32 mmol, 1.5 eq) were dissolved in DMF (15 mL) and stirred for 17 h at room temperature. Purification of the obtained brownish liquid was done by column chromatography (Cy/EtOAc, 10:1, (v:v), by sampling the spot at R_f = 0.58 (Cy/EtOAc, 5:1, (v:v))). Yield: 577.5 mg (83 %) white solid.

TLC: R_f = 0.58 (Cy/EtOAc, 5:1, (v:v))

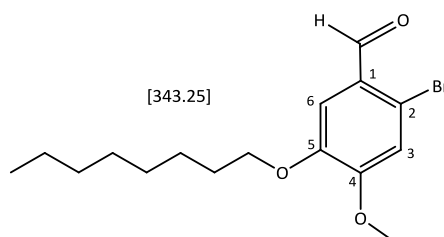


¹H-NMR: (δ, 20°C, CDCl₃, 300.36 MHz): 10.14 (s, 1H, CHO), 7.37 (s, 1H, ph³), 7.01 (s, 1H, ph⁶), 4.01 (t, 2H, ³J_{HH} = 6.8 Hz, OCH₂(CH₂)₄CH₃), 3.91 (s, 3H, OCH₃), 1.80 (m, 2H, OCH₂CH₂(CH₂)₃CH₃), 1.42 (m, 2H, O(CH₂)₂CH₂(CH₂)₂CH₃), 1.31 (m, 4H, O(CH₂)₃(CH₂)₂CH₃), 0.88 (m, 3H, O(CH₂)₅CH₃)

5.2.2.4 2-Bromo-5-octyloxyoxy-4-methoxy benzaldehyde

2-Bromo-4-methoxy-5-octyloxyoxy benzaldehyde was synthesized as mentioned above, using 2-bromo-5-hydroxy-4-methoxybenzaldehyde (517.2 mg, 2.24 mmol, 1 eq), K_2CO_3 (618.7 mg, 4.48 mmol, 2 eq), Cs_2CO_3 (36.5 mg, 0.11 mmol, 0.05 eq) and 1-iodooctane (606.3 μ L, 3.36 mmol, 1.5 eq). The remaining brown oil was purified by column chromatography (Cy/EtOAc, 10:1, (v:v), by sampling the spot with $R_f = 0.67$ (Cy/EtOAc, 5:1, (v:v))). Yield: 636.0 mg (83 %) white-brownish solid.

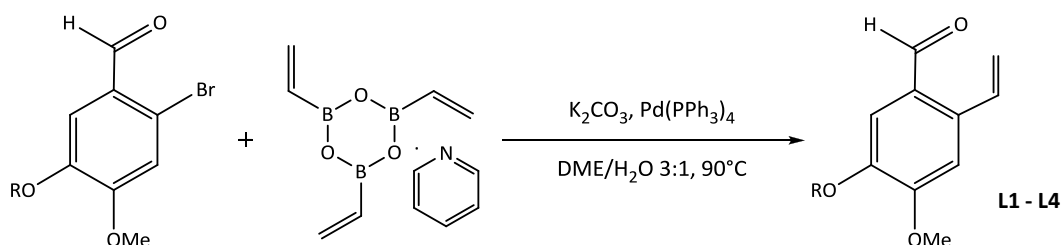
TLC: $R_f = 0.67$ (Cy/EtOAc, 5:1, (v:v))



1H -NMR: (δ , 20°C, $CDCl_3$, 300.36 MHz): 10.13 (s, 1H, CHO), 7.36 (s, 1H, ph^3), 7.01 (s, 1H, ph^6), 4.00 (t, 2H, $^3J_{HH} = 6.8$ Hz, $OCH_2(CH_2)_6CH_3$), 3.91 (s, 3H, OCH_3), 1.80 (m, 2H, $OCH_2CH_2(CH_2)_5CH_3$), 1.41 (m, 2H, $O(CH_2)_2CH_2(CH_2)_4CH_3$), 1.25 (m, 6H, $O(CH_2)_4(CH_2)_3CH_3$), 0.85 (t, 3H, $^3J_{HH} = 6.8$ Hz, $O(CH_2)_7CH_3$)

5.2.3 Vinylations (5-Alkoxy-4-methoxy-2-vinyl benzaldehydes)

All ligands were prepared via Suzuki coupling of the 5-alkoxy-2-bromo-4-methoxy benzaldehyde precursors mentioned above (see part 5.2.2).



Scheme 12. Reaction scheme for the Suzuki coupling reaction⁹

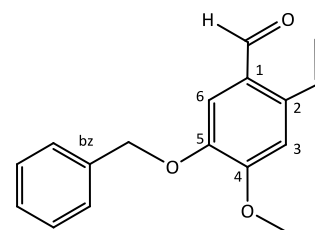
5.2.3.1 5-Benzyloxy-4-methoxy-2-vinyl benzaldehyde (**L1**)

For the preparation of **L1** 5-benzyloxy-2-bromo-4-methoxy benzaldehyde (375.4 mg, 1.17 mmol, 1.0 eq), K_2CO_3 (483.9 mg, 3.51 mmol, 3.0 eq) and vinylboronic anhydride pyridine complex (309.5 mg, 1.29 mmol, 1.1 eq) were dissolved in degassed DME/H_2O 3:1 (v:v) (7 mL) under nitrogen atmosphere and heated to $90^\circ C$. Vinylation was started by adding $Pd(PPh_3)_4$ (21.9 mg, 0.02 mmol, 0.03 eq) and stirred for 16 h at $90^\circ C$. As full conversion was not reached, again $Pd(PPh_3)_4$ (0.03 eq) was added and the reaction mixture was stirred for another 5 h. The reaction solution was diluted by adding H_2O (10 mL) and CH_2Cl_2 (10 mL). Insoluble components were removed via filtration through glass wool. The organic layer was washed with aqueous HCl (5 %, 3 x 15 mL), aqueous $NaHCO_3$ (saturated, 3 x 15 mL) and H_2O (3 x 15 mL). The CH_2Cl_2 phase was dried with Na_2SO_4 , filtered, evaporated and dried in vacuo. The remaining brownish solid was purified via column chromatography (Cy/EtOAc, 10:1, (v:v), by sampling the spot with $R_f = 0.25$ (Cy/EtOAc, 5:1, (v:v))). Yield: 239.8 mg (77 %) white solid (after recrystallization from hot Cy colourless needles were received).

TLC: $R_f = 0.25$ (Cy/EtOAc, 5:1, (v:v))

Elementary analysis: $C_{17}O_3H_{16}$ [268.31]

75.60 % C, 6.10 % H (calculated: 76.10 % C, 6.01 % H, 17.89 % O)



¹H-NMR: (δ , 20°C, CDCl₃, 300.36 MHz): 10.21 (s, 1H, CHO), 7.51-7.28 (m, 7H, CHCH₂, ph⁵, OCH₂(C₆H₅)), 6.99 (s, 1H, ph⁶), 5.64 (dd, 1H, ³J_{HHtrans} = 17.3 Hz, ²J_{HH} = 0.9 Hz, CHCH₂), 5.49 (dd, 1H, ³J_{HHcis} = 11.0 Hz, ²J_{HH} = 0.9 Hz, CHCH₂), 5.20 (s, 2H, CH₂^{bz}), 3.98 (s, 3H, OCH₃)

¹³C-NMR: (δ , 20°C, CDCl₃, 75.53 MHz): 190.04 (1C, CHO), 154.48 (1C, ph⁴), 148.22 (1C, ph⁵), 136.46 (1C, bz¹), 136.44 (1C, ph²), 132.44 (1C, CHCH₂), 128.76 (2C, bz^{3,5}), 128.25 (1C, bz⁴), 127.63 (2C, bz^{2,6}), 126.39 (1C, ph¹), 118.80 (1C, CHCH₂), 112.98 (1C, ph⁶), 109.46 (1C, ph³), 71.05 (1C, CH₂^{bz}), 56.25 (1C, OCH₃)

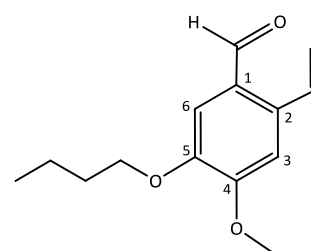
5.2.3.2 5-Butyloxy-4-methoxy-2-vinyl benzaldehyde (**L2**)

For the synthesis of **L2** 2-bromo-5-butyloxy-4-methoxy benzaldehyde (498.0 mg, 1.73 mmol, 1.0 eq), K₂CO₃ (718.1 mg, 5.20 mmol, 3.0 eq), Cs₂CO₃ (tip of a spatula) and vinylboronic anhydride pyridine complex (459.7 mg, 1.91 mmol, 1.1 eq) were dissolved in degassed DME/H₂O 3:1 (v:v) (10 mL) under inert conditions and heated to 90°C. Vinylation was started by adding Pd(PPh₃)₄ (60.1 mg, 0.05 mmol, 0.03 eq) and stirred for 25 h at 90°C. Complete conversion was not achieved, although Pd(PPh₃)₄ (0.03 eq) was added again after 20 h. The work-up of the reaction mixture was performed analogously to the benzyloxy derivative, but CH₂Cl₂ was replaced by Et₂O due to better phase separation. The obtained yellow-brownish liquid was purified via column chromatography (Cy/EtOAc, 20:1, (v:v)), by sampling the spot with R_f = 0.37 (Cy/EtOAc, 5:1, (v:v)). Yield: 331.6 mg (82 %) colourless needles.

TLC: R_f = 0.37 (Cy/EtOAc, 5:1, (v:v))

Elementary analysis: C₁₄O₃H₁₈ [234.29]

71.62 % C, 7.82 % H (calculated: 71.77 % C, 7.74 % H, 20.49 % O)



¹H-NMR: (δ , 20°C, CDCl₃, 300.36 MHz): 10.24 (s, 1H, CHO), 7.43 (dd, 1H, ³J_{HHcis} = 10.9 Hz, ³J_{HHtrans} = 17.3 Hz, CHCH₂), 7.35 (s, 1H, ph⁵), 6.96 (s, 1H, ph⁶), 5.62 (dd, 1H, ³J_{HHtrans} = 17.3 Hz, ²J_{HH} = 0.9 Hz, CHCH₂), 5.47 (dd, 1H, ³J_{HHcis} = 11.0 Hz, ²J_{HH} = 0.9 Hz, CHCH₂), 4.07 (t, 2H, ³J_{HH} = 6.8 Hz, OCH₂(CH₂)₂CH₃), 3.98 (s, 3H, OCH₃), 1.84 (m, 2H, OCH₂CH₂CH₂CH₃), 1.50 (m, 2H, O(CH₂)₂CH₂CH₃), 0.98 (t, 3H, ³J_{HH} = 7.4 Hz, O(CH₂)₃CH₃)

¹³C-NMR: (δ , 20°C, CDCl₃, 75.53 MHz): 190.14 (1C, CHO), 154.25 (1C, ph⁴), 148.68 (1C, ph⁵), 136.02 (1C, ph²), 132.39 (1C, CHCH₂), 126.44 (1C, ph¹), 118.63 (1C, CHCH₂), 111.75 (1C, ph⁶), 109.24 (1C, ph³), 68.94 (1C, OCH₂(CH₂)₂CH₃), 56.24 (1C, OCH₃), 31.17 (1C, , OCH₂CH₂CH₂CH₃), 19.29 (1C, , O(CH₂)₂CH₂CH₃), 13.95 (1C, O(CH₂)₃CH₃)

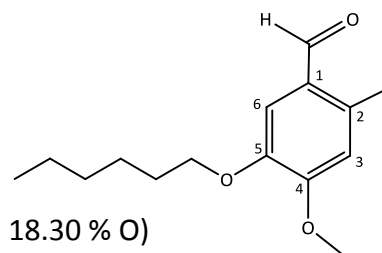
5.2.3.3 5-Hexyloxy-4-methoxy-2-vinyl benzaldehyde (**L3**)

The preparation of 5-hexyloxy-4-methoxy-2-vinyl benzaldehyde (**L3**) was performed as mentioned above, using 2-Bromo-5-hexyloxy-4-methoxy benzaldehyde (577.5 mg, 1.83 mmol, 1.0 eq), K₂CO₃ (759.6 mg, 5.50 mmol, 3.0 eq), Cs₂CO₃ (tip of a spatula) and vinylboronic anhydride pyridine complex (485.1 mg, 2.02 mmol, 1.1 eq). Pd(PPh₃)₄ (63.4 mg, 0.06 mmol, 0.03 eq) was added and the reaction was stirred for 20 h at 90°C. Purification of the remaining brown oil was done by column chromatography (Cy/EtOAc, 20:1, (v:v), by sampling the spot with R_f = 0.39 (Cy/EtOAc, 5:1, (v:v))). Yield: 417.6 mg (87 %) yellowish oil.

TLC: R_f = 0.39 (Cy/EtOAc, 5:1, (v:v))

Elementary analysis: C₁₆O₃H₂₂ [262.35]

72.09 % C, 8.56 % H, 0.43 % N (calculated: 73.25 % C, 8.45 % H, 18.30 % O)



¹H-NMR: (δ , 20°C, CDCl₃, 300.36 MHz): 10.24 (s, 1H, CHO), 7.43 (dd, 1H, ³J_{HHcis} = 10.9 Hz, ³J_{HHtrans} = 17.3 Hz, CHCH₂), 7.35 (s, 1H, ph³), 6.96 (s, 1H, ph⁶), 5.63 (dd, 1H, ³J_{HHtrans} = 17.3 Hz, ²J_{HH} = 0.9 Hz, CHCH₂), 5.48 (dd, 1H, ³J_{HHcis} = 11.0 Hz, ²J_{HH} = 0.8 Hz, CHCH₂), 4.07 (t, 2H, ³J_{HH} = 6.9 Hz, OCH₂(CH₂)₄CH₃), 3.96 (s, 3H, OCH₃), 1.86 (m, 2H, OCH₂CH₂(CH₂)₃CH₃), 1.46 (m, 2H, O(CH₂)₂CH₂(CH₂)₂CH₃), 1.34 (m, 4H, O(CH₂)₂CH₂(CH₂)₂CH₃), 0.90 (t, 3H, ³J_{HH} = 7.0 Hz, O(CH₂)₅CH₃)

¹³C-NMR: (δ , 20°C, CDCl₃, 75.53 MHz): 190.17 (1C, CHO), 154.25 (1C, ph⁴), 148.68 (1C, ph⁵), 136.03 (1C, ph²), 132.40 (1C, CHCH₂), 126.45 (1C, ph¹), 118.66 (1C, CHCH₂), 111.75 (1C, ph⁶), 109.24 (1C, ph³), 69.27 (1C, OCH₂(CH₂)₄CH₃), 56.25 (1C, OCH₃), 31.67 (1C, OCH₂CH₂(CH₂)₃CH₃), 29.09 (1C, O(CH₂)₂CH₂(CH₂)₂CH₃), 25.72 (1C, O(CH₂)₃CH₂CH₂CH₃), 22.70 (1C, O(CH₂)₄CH₂CH₃), 14.15 (1C, O(CH₂)₅CH₃)

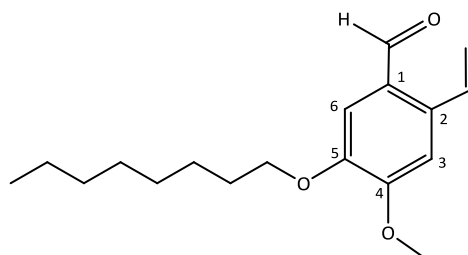
5.2.3.4 4-Methoxy-5-octyloxy-2-vinyl benzaldehyde (**L4**)

The synthesis of 4-methoxy-5-octyloxy-2-vinyl benzaldehyde (**L4**) was performed analogously to prior derivatives using 2-bromo-4-methoxy-5-octyloxyoxy benzaldehyde (636.0 mg, 1.85 mmol, 1.0 eq), K_2CO_3 (768.2 mg, 5.60 mmol, 3.0 eq), Cs_2CO_3 (tip of a spatula) and vinylboronic anhydride pyridine complex (490.6 mg, 2.04 mmol, 1.1 eq). $Pd(PPh_3)_4$ (64.1 mg, 0.06 mmol, 0.03 eq) was added and the reaction was stirred for 20 h at $90^\circ C$, complete conversion was reached. The resulting residue (brown oil) was purified by column chromatography (Cy/EtOAc, 20:1, (v:v), by sampling the spot with $R_f = 0.45$ (Cy/EtOAc, 5:1, (v:v))). Yield: 518.7 mg (96 %) yellowish oil.

TLC: $R_f = 0.45$ (Cy/EtOAc, 5:1, (v:v))

Elementary analysis: $C_{18}O_3H_{26}$ [290.40]

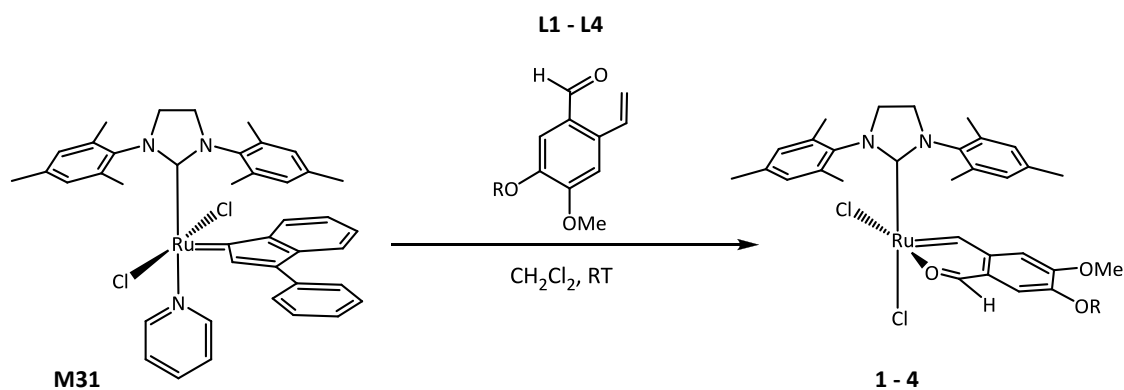
73.62 % C, 9.00 % H, 0.22 % N (calculated: 74.45 % C, 9.02 % H, 16.53 % O)



1H -NMR: (δ , $20^\circ C$, $CDCl_3$, 300.36 MHz): 10.24 (s, 1H, CHO), 7.43 (dd, 1H, $^3J_{HHcis} = 11.0$ Hz, $^3J_{HHtrans} = 17.3$ Hz, CHCH₂), 7.35 (s, 1H, ph³), 6.96 (s, 1H, ph⁶), 5.63 (dd, 1H, $^3J_{HHtrans} = 17.3$ Hz, $^2J_{HH} = 1.0$ Hz, CHCH₂), 5.47 (dd, 1H, $^3J_{HHcis} = 11.0$ Hz, $^2J_{HH} = 1.0$ Hz, CHCH₂), 4.07 (t, 2H, $^3J_{HH} = 6.9$ Hz, $OCH_2(CH_2)_6CH_3$), 3.96 (s, 3H, OCH_3), 1.86 (m, 2H, $OCH_2CH_2(CH_2)_5CH_3$), 1.46 (m, 2H, $O(CH_2)_2CH_2(CH_2)_4CH_3$), 1.28 (m, 6H, $O(CH_2)_4(CH_2)_3CH_3$), 0.88 (t, 3H, $^3J_{HH} = 6.6$ Hz, $O(CH_2)_7CH_3$)

^{13}C -NMR: (δ , $20^\circ C$, $CDCl_3$, 75.53 MHz): 190.18 (1C, CHO), 154.25 (1C, ph⁴), 148.68 (1C, ph⁵), 136.03 (1C, ph²), 132.41 (1C, CHCH₂), 126.45 (1C, ph¹), 118.66 (1C, CHCH₂), 111.75 (1C, ph⁶), 109.24 (1C, ph³), 69.28 (1C, $OCH_2(CH_2)_6CH_3$), 56.25 (1C, OCH_3), 31.93 (1C, $OCH_2CH_2(CH_2)_5CH_3$), 29.45 (1C, $O(CH_2)_2CH_2(CH_2)_4CH_3$), 29.33 (1C, $O(CH_2)_3CH_2(CH_2)_3CH_3$), 29.12 (1C, $O(CH_2)_4CH_2(CH_2)_2CH_3$), 26.05 (1C, $O(CH_2)_5CH_2CH_2CH_3$), 22.78 (1C, $O(CH_2)_6CH_2CH_3$), 14.23 (1C, $O(CH_2)_7CH_3$)

5.2.4 Ruthenium(II) Complexes



Scheme 13. Synthesis of Ru(II)-complexes from **M31**

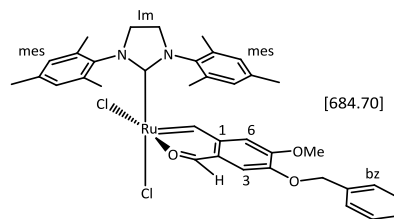
M31 (1.0 eq) was dissolved in dry degassed CH_2Cl_2 in a Schlenk flask under nitrogen atmosphere. The requested 5-alkoxy-4-methoxy-2-vinyl benzaldehyde (1.1 to 1.2 eq) was added and the reaction solution was stirred at room temperature under nitrogen atmosphere for 3-4 h until the color turned from deep red/brown to deep green (monitored via TLC).⁹ The solvent was evaporated to 1-2 mL and the complex was precipitated and washed with *n*-pentane. The green powder was dried in vacuo and purified by column chromatography.

5.2.4.1 Dichloro(4-benzyloxy-2-formyl-5-methoxybenzylidene- $\kappa^2(\text{C},\text{O})$)(1,3-bis(2,4,6-trimethylphenyl)-4,5-dihydroimidazol-2-ylidene)ruthenium (**1**)

Complex **1** was prepared analogously to the general procedure mentioned above. **M31** (373.9 mg, 0.50 mmol, 1 eq) and 5-benzyloxy-4-methoxy-2-vinyl benzaldehyde (161.0 mg, 0.60 mmol, 1.2 eq) were dissolved in CH_2Cl_2 (7 mL). Purification was done by column chromatography, using CH_2Cl_2 and $\text{CH}_2\text{Cl}_2/\text{MeOH}$, 20:1-10:1, (v:v). Yield: 213.2 mg (62 %) green microcrystals.

TLC: $R_f = 0.62$ ($\text{CH}_2\text{Cl}_2/\text{MeOH}$, 10:1, (v:v))

¹H-NMR: (δ , 20°C, CDCl₃, 300.36 MHz): 18.59 (s, 1H, Ru=CH), 9.59 (s, 1H, CHO), 7.52 (s, 1H, bz), 7.50 (s, 1H, bz), 7.39-7.24 (m, 3H^{bz}, 1H^{mes}), 7.20 (bs, 1H, mes), 6.95 (s, 1H, ph⁶), 6.82 (bs, 1H, mes), 6.54 (s, 1H, ph³), 5.48 (bs, 1H, mes), 5.15 (m, 1H, CH₂^{bz}), 5.07 (m, 1H, CH₂^{bz}), 4.28-3.43 (m, 4H, Im), 3.95 (s, 3H, OCH₃), 2.70 (s, 3H, CH₃^{mes}), 2.45 (s, 6H, CH₃^{mes}), 2.00 (s, 3H, CH₃^{mes}), 1.58 (s, 3H, CH₃^{mes}), 0.88 (s, 3H, CH₃^{mes})



Signals for **1b**:

¹H-NMR of complex **1** in methanol-d₄ gave a spectrum of very poor quality (due to bad solubility), anyway a carbene resonance at 19.22 ppm was observed which indicates a similar cationic structure as found for complexes **2-4** (compare **2b**, page 61).

¹³C-NMR: (δ , 20°C, CDCl₃, 125.72 MHz): 283.65 (1C, Ru=CH), 213.85 (1C_q, CNN), 204.11 (1C, CHO), 156.75 (1C_q, ph⁵), 147.00 (1C_q, ph⁴), 140.39, 139.94 (2C_q, C^{mes-N}), 138.18, 137.94, 137.77, 135.20, 135.42, 131.63 (6C_q, C^{mes}), 130.94, 130.08, 129.29, 128.40 (4C, mes), 136.02 (1C_q, bz¹), 130.81 (1C_q, ph¹), 128.65, 128.09 (4C, bz^{2,3,5,6}), 128.18 (1C, bz⁴), 121.84 (1C_q, ph²), 120.02 (1C_q, ph³), 108.09 (1C_q, ph⁶), 70.45 (1C, CH₂^{bz}), 56.31 (1C, OCH₃), 53.58, 50.98 (2C, Im), 21.55, 20.70, 20.30, 18.46, 18.43, 16.62 (6C, CH₃^{mes}),

5.2.4.2 Dichloro(4-butyloxy-2-formyl-5-methoxybenzylidene- $\kappa^2(C,O)$)(1,3-bis(2,4,6-trimethylphenyl)-4,5-dihydroimidazol-2-ylidene)ruthenium (**2**)

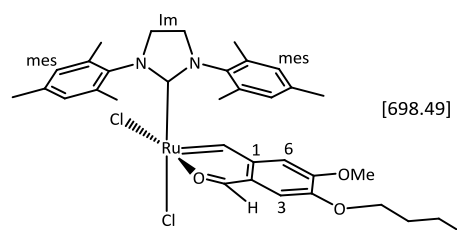
Pre-synthesis in NMR-tube

M31 (5.0 mg, 6.69·10⁻³ mmol, 1.0 eq) and 5-butyloxy-4-methoxy-2-vinyl benzaldehyde (1.7 mg, 7.36·10⁻³ mmol, 1.1 eq) were dissolved in CDCl₃ (0.6 mL). The formation of the ruthenium carbene species was detected via ¹H-NMR (300.36 MHz, 20°C) recording a spectrum within the 8500 MHz region.

Complex **2** was synthesized according the general procedure above using **M31** (250.0 mg, 0.33 mmol, 1.0 eq) and 5-butyloxy-4-methoxy-2-vinyl benzaldehyde (90.1 mg, 0.38 mmol, 1.15 eq) in 10 mL CH₂Cl₂. The precipitated crude product was purified by column

chromatography (CH₂Cl₂/MeOH, 10:1, (v:v)) by sampling the spot with R_f = 0.45 (CH₂Cl₂/MeOH, 10:1, (v:v)) as main product (*cis*-dichloro species). Yield: 151.8 mg (65 %) green crystals. The spot with R_f = 0.10 (CH₂Cl₂/MeOH, 10:1, (v:v)) was isolated as side product **2a** (cationic species). Yield: 38.0 mg (16 %) deep green powder. Within the main fraction, a third carbene species (**2b**) appeared at 19.16 ppm (approx. 10%). Isolation of this complex was not feasible, but ¹H NMR measurements of the main fraction in methanol-d₄ show a complete rearrangement, most likely to this third structure.

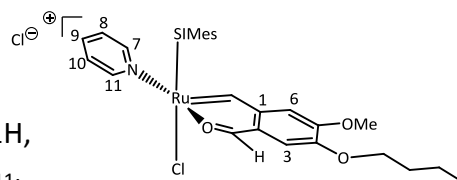
TLC: R_f = 0.55 (CH₂Cl₂/MeOH, 10:1, (v:v))



¹H-NMR: (δ, 20°C, CDCl₃, 300.36 MHz): 18.43 (s, 1H, Ru=CH), 9.72 (s, 1H, CHO), 7.29 (bs, 1H, mes), 7.18 (bs, 1H, mes), 7.00 (s, 1H, ph⁶), 6.90 (bs, 1H, mes), 6.53 (s, 1H, ph³), 5.95 (bs, 1H, mes), 4.33-3.49 (m, 4H, Im), 4.01-3.78 (t, 2H, OCH₂(CH₂)₂CH₃), 3.93 (s, 3H, OCH₃), 2.72 (s, 3H, CH₃^{mes}), 2.50 (s, 3H, CH₃^{mes}), 2.44 (s, 6H, CH₃^{mes}), 2.06 (s, 3H, CH₃^{mes}), 1.80 (m, 2H, OCH₂CH₂CH₂CH₃), 1.52 (m, 2H, O(CH₂)₂CH₂CH₃), 1.05 (s, 3H, CH₃^{mes}), 0.99 (t, 3H, ³J_{HH} = 7.4 Hz, O(CH₂)₃CH₃).

¹³C-NMR: (δ, 20°C, CDCl₃, 125.72 MHz): 284.09 (1C, Ru=CH), 213.91 (1C_q, CNN), 204.20 (1C, CHO), 156.47 (1C_q, ph⁵), 148.49 (1C_q, ph⁴), 140.29, 139.87 (2C_q, C^{mes-N}), 138.24, 138.20, 137.78, 135.60, 135.19, 131.63, (6C_q, C^{mes}), 130.86, 130.05, 129.49, 128.42 (4C, mes), 130.82 (1C_q, ph¹), 122.22 (1C_q, ph²), 118.34 (1C_q, ph³), 108.09 (1C_q, ph⁶), 69.35 (1C, OCH₂(CH₂)₂CH₃), 56.25 (1C, OCH₃), 51.04, 50.97 (2C, Im), 31.11 (1C, OCH₂CH₂CH₂CH₃), 21.50, 20.83, 20.24, 18.50, 18.41, 16.78 (6C, CH₃^{mes}), 19.34 (1C, O(CH₂)₂CH₂CH₃), 14.11 (1C, O(CH₂)₃CH₃)

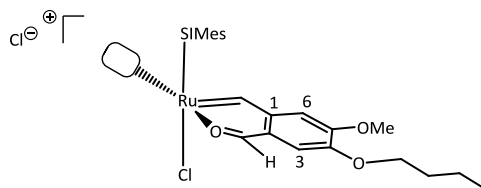
Signals for **2a**:



¹H-NMR: (δ, 20°C, CDCl₃, 300.36 MHz): 17.80 (s, 1H, Ru=CH), 9.93 (s, 1H, CHO), 8.59 (d, 2H, ⁴J_{HH} = 5.0 Hz, py^{7,11}), 7.76 (t, 1H, ³J_{HH} = 7.0 Hz, py⁹), 7.60 (s, 1H, ph⁶), 7.47 (s, 1H, ph³), 7.33 (dd, 2H, ³J_{HH} = 5.9 Hz, py^{8,10}), 6.96 (s, 2H, mes), 6.44 (s, 2H, mes), 4.23 (m, 1H, OCH₂(CH₂)₂CH₃), 4.11 (m, 1H, OCH₂(CH₂)₂CH₃), 4.08 (s, 3H, OCH₃), 3.96 (bs, 4H, Im), 2.66 (s, 6H, CH₃^{mes}), 2.13 (s, 6H, CH₃^{mes}), 1.88 (m, 2H, OCH₂CH₂CH₂CH₃), 1.64 (s, 6H, CH₃^{mes}), 1.53 (m, 2H, O(CH₂)₂CH₂CH₃), 0.99 (t, 3H, ³J_{HH} = 7.3 Hz, O(CH₂)₃CH₃).

Signals for **2b**:

^1H (δ , 20°C, methanol- d_4 , referenced to TMS-standard, 300.36 MHz): 19.11 (s, 1H, Ru=CH), 9.96 (s, 1H, CHO), 7.66 (s, 1H, ph⁶), 7.14 (s, 2H, mes), 6.96 (s, 1H, ph³), 6.67 (s, 2H, mes), 4.29 (m, 1H, OCH₂(CH₂)₂CH₃), 4.19 (m, 1H, OCH₂(CH₂)₂CH₃), 4.08 (s, 3H, OCH₃), 3.84 (s, 4H, Im), 2.42 (s, 6H, CH₃^{mes}), 2.30 (s, 6H, CH₃^{mes}), 1.94 (s, 6H, CH₃^{mes}), 1.91 (m, 2H, OCH₂CH₂CH₂CH₃), 1.60 (m, 2H, O(CH₂)₂CH₂CH₃), 1.05 (t, 3H, ³J_{HH} = 7.4 Hz, O(CH₂)₃CH₃).



5.2.4.3 Dichloro(2-formyl-4-hexyloxy-5-methoxybenzylidene- $\kappa^2(\text{C},\text{O})$)(1,3-bis(2,4,6-trimethylphenyl)-4,5-dihydroimidazol-2-ylidene)ruthenium (**3**)

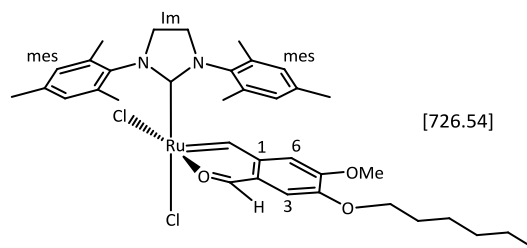
Pre-synthesis in NMR-tube

M31 (5.0 mg, $6.69 \cdot 10^{-3}$ mmol, 1.0 eq) and 5-hexyloxy-4-methoxy-2-vinyl benzaldehyde (1.9 mg, $7.36 \cdot 10^{-3}$ mmol, 1.1 eq) were dissolved in CDCl₃ (0.6 mL). The formation of the ruthenium carbene species was detected via ^1H -NMR (300.36 MHz, 20°C) recording a spectrum within the 8500 MHz region.

The formation of complex **3** was made following the mentioned steps above. **M31** (250.1 mg, 0.33 mmol, 1.0 eq) and 5-hexyloxy-4-methoxy-2-vinyl benzaldehyde (100.9 mg, 0.38 mmol, 1.15 eq) were dissolved in 10 mL CH₂Cl₂. The obtained green powder was purified by column chromatography using CH₂Cl₂/MeOH, 20:1 and 10:1, (v:v). Three fractions were isolated by sampling the spots with $R_f = 0.57$ (*cis*-dichloro species, main product), $R_f = 0.43$ (containing the *cis*-dichloro species and two not identified carbene species) and $R_f = 0.25$ (cationic species) (CH₂Cl₂/MeOH, 10:1, (v:v)). Yield: 128.2 mg (53 %) green powder.

TLC: $R_f = 0.55$ (CH₂Cl₂/MeOH, 10:1, (v:v))

¹H-NMR: (δ , 20°C, CDCl₃, 300.36 MHz): 18.44 (s, 1H, Ru=CH), 9.72 (s, 1H, CHO), 7.29 (bs, 1H, mes), 7.19 (bs, 1H, mes), 7.01 (s, 1H, ph⁶), 6.91 (bs, 1H, mes), 6.56 (s, 1H, ph³), 5.97 (bs, 1H, mes), 4.31-3.50 (m, 4H, Im), 4.03-3.79 (t, 2H,



OCH₂(CH₂)₄CH₃), 3.93 (s, 3H, OCH₃), 2.74 (s, 3H, CH₃^{mes}), 2.52 (s, 3H, CH₃^{mes}), 2.43 (s, 6H, CH₃^{mes}), 2.08 (s, 3H, CH₃^{mes}), 1.83 (m, 2H, OCH₂CH₂(CH₂)₃CH₃), 1.52 (m, 2H, O(CH₂)₂CH₂(CH₂)₂CH₃), 1.37 (m, 4H, O(CH₂)₃(CH₂)₂CH₃), 1.06 (s, 3H, CH₃^{mes}), 0.93 (t, 3H, ³J_{HH} = 6.7 Hz, O(CH₂)₅CH₃)

¹³C-NMR: (δ , 20°C, CDCl₃, 75.53 MHz): 284.06 (1C, Ru=CH), 214.03 (1C_q, CNN), 204.11 (1C, CHO), 156.61 (1C_q, ph⁵), 148.59 (1C_q, ph⁴), 140.37, 139.93 (2C_q, C^{mes-N}), 138.35, 138.22, 137.79, 135.24, 135.67, 131.61 (6C_q, C^{mes}), 130.94 (1C_q, ph¹), 130.09, 129.78, 129.58, 128.46 (4C, mes), 122.23 (1C_q, ph²), 118.30 (1C_q, ph³), 108.19 (1C_q, ph⁶), 69.71 (1C, OCH₂(CH₂)₄CH₃), 56.28 (1C, OCH₃), 51.01 (2C, Im), 31.74 (1C, OCH₂CH₂(CH₂)₃CH₃), 29.04 (1C, O(CH₂)₂CH₂(CH₂)₂CH₃), 25.89 (1C, O(CH₂)₃CH₂CH₂CH₃), 22.77 (1C, O(CH₂)₄CH₂CH₃), 21.52, 20.88, 20.26, 18.53, 18.39, 16.78 (6C, CH₃^{mes}), 14.19 (1C, O(CH₂)₅CH₃)

5.2.4.4 Dichloro(2-formyl-5-methoxy-4-octyloxybenzylidene- κ^2 (C,O))(1,3-bis(2,4,6-trimethylphenyl)-4,5-dihydroimidazol-2-ylidene)ruthenium (**4**)

Pre-synthesis in NMR-tube

M31 (5.0 mg, 6.69·10⁻³ mmol, 1.0 eq) and 4-methoxy-5-octyloxy-2-vinyl benzaldehyde (2.1 mg, 7.36·10⁻³ mmol, 1.1 eq) were dissolved in CDCl₃ (0.6 mL). The formation of the ruthenium carbene species was detected via ¹H-NMR (300.36 MHz, 20°C) recording a spectrum within the 8500 MHz region.

Synthesis of complex **4** was done using the same operation steps as for previous structures. M31 (250.0 mg, 0.33 mmol, 1.0 eq) and 5-hexyloxy-4-methoxy-2-vinyl benzaldehyde (100.9 mg, 0.38 mmol, 1.15 eq) were dissolved in 10 mL CH₂Cl₂. Purification of the remaining green powder was done by column chromatography using CH₂Cl₂/MeOH, 20:1 and 10:1, (v:v) as eluent. The *cis*-dichloro complex could be isolated by sampling the spot with R_f = 0.50 (main

product) and cationic species by sampling the spot with $R_f = 0.05$ (side product) ($\text{CH}_2\text{Cl}_2/\text{MeOH}$, 10:1, (v:v)). Yield: 185.3 mg (73 %) green powder.

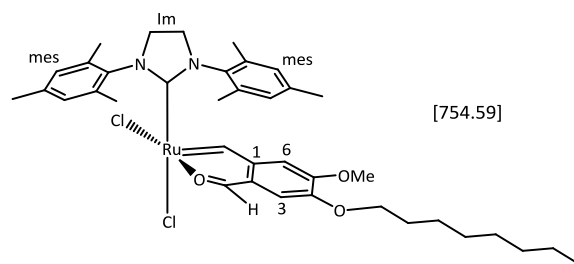
TLC: $R_f = 0.57$ ($\text{CH}_2\text{Cl}_2/\text{MeOH}$, 10:1, (v:v))

$^1\text{H-NMR}$: (δ , 20°C, CDCl_3 , 300.36 MHz): 18.44

(s, 1H, $\text{Ru}=\text{CH}$), 9.73 (s, 1H, CHO), 7.29 (bs, 1H, mes), 7.19 (bs, 1H, mes), 7.02 (s, 1H, ph^6),

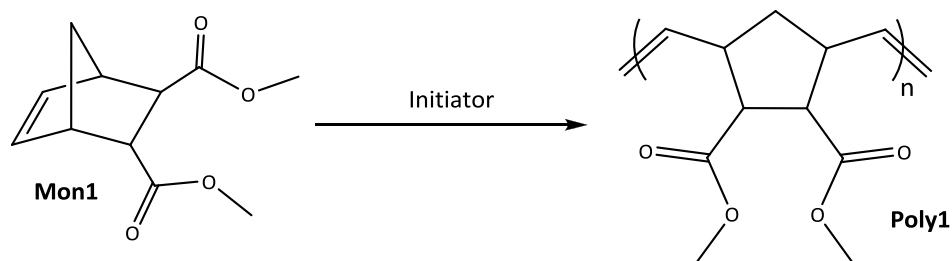
6.91 (bs, 1H, mes), 6.56 (s, 1H, ph^3), 5.98 (bs, 1H, mes), 4.31-3.49 (m, 4H, Im), 4.05-3.79 (t, 2H, $\text{OCH}_2(\text{CH}_2)_4\text{CH}_3$), 3.93 (s, 3H, OCH_3), 2.73 (s, 3H, CH_3^{mes}), 2.52 (s, 3H, CH_3^{mes}), 2.43 (s, 6H, CH_3^{mes}), 2.08 (s, 3H, CH_3^{mes}), 1.83 (m, 2H, $\text{OCH}_2\text{CH}_2(\text{CH}_2)_5\text{CH}_3$), 1.50 (m, 2H, $\text{O}(\text{CH}_2)_2\text{CH}_2(\text{CH}_2)_4\text{CH}_3$), 1.42-1.23 (m, 8H, $\text{O}(\text{CH}_2)_3(\text{CH}_2)_4\text{CH}_3$), 1.06 (s, 3H, CH_3^{mes}), 0.90 (t, 3H, $^3J_{\text{HH}} = 6.6$ Hz, $\text{O}(\text{CH}_2)_5\text{CH}_3$)

$^{13}\text{C-NMR}$: (δ , 20°C, CDCl_3 , 75.53 MHz): 284.09 (1C, $\text{Ru}=\text{CH}$), 214.01 (1C_q, CNN), 204.09 (1C, CHO), 156.64 (1C_q, ph^5), 148.60 (1C_q, ph^4), 140.38, 139.92 (2C_q, $\text{C}^{\text{mes-N}}$), 138.35, 138.20, 137.82, 135.22, 135.68, 131.58 (6C_q, C^{mes}), 130.96 (1C_q, ph^1), 130.06, 129.77, 129.58, 128.46 (4C, mes), 122.21 (1C_q, ph^2), 118.27 (1C_q, ph^3), 108.22 (1C_q, ph^6), 69.72 (1C, $\text{OCH}_2(\text{CH}_2)_6\text{CH}_3$), 56.29 (1C, OCH_3), 51.01 (2C, Im), 31.95 (1C, $\text{OCH}_2\text{CH}_2(\text{CH}_2)_5\text{CH}_3$), 29.54 (1C, $\text{O}(\text{CH}_2)_2\text{CH}_2(\text{CH}_2)_4\text{CH}_3$), 29.41 (1C, $\text{O}(\text{CH}_2)_3\text{CH}_2(\text{CH}_2)_3\text{CH}_3$), 29.06 (1C, $\text{O}(\text{CH}_2)_4\text{CH}_2(\text{CH}_2)_2\text{CH}_3$), 26.20 (1C, $\text{O}(\text{CH}_2)_5\text{CH}_2\text{CH}_2\text{CH}_3$), 22.80 (1C, $\text{O}(\text{CH}_2)_6\text{CH}_2\text{CH}_3$), 21.51, 20.89, 20.26, 18.52, 18.42, 16.78 (6C, CH_3^{mes}), 14.24 (1C, $\text{O}(\text{CH}_2)_7\text{CH}_3$)



5.2.5 Ring Opening Metathesis Polymerization (ROMP)

5.2.5.1 ROMP of **Mon1** ($M:I = 300$)



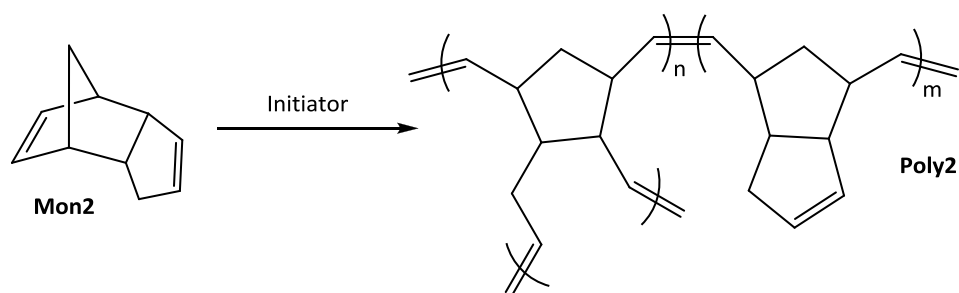
Scheme 14. ROM Polymerization of dimethyl-5-norbornene-2,3-dicarboxylate (**Mon1**)

For a typical polymerization procedure a concentration of 0.1 M in respect of the monomer was used ($M:I = 300$). **Mon1** (100.0 mg, 0.48 mmol, 300 eq) was dissolved in dry degassed solvent and brought to the required temperature under nitrogen atmosphere. Polymerization was started by adding the initiator (1.0 eq, from 4 mg/mL stock solution) and the reaction was monitored via TLC. After complete conversion of the monomer, the reaction solution was evaporated to 1-2 mL and the polymer was precipitated in MeOH (50 mL, iced) and dried in vacuo. The obtained polymer (**Poly1**) was analysed via GPC. This standard polymerization protocol was performed at RT and 40°C in CH_2Cl_2 and at 80°C in toluene.

5.2.5.2 ROMP of **Mon1** in NMR tube ($M:I = 10$)

1 eq initiator (3 mg, 0.004 mmol) was dissolved in 0.4 mL CDCl_3 and the required amount of **Mon1** was injected (10 eq, 0.043 mmol in 0.3 mL CDCl_3). The propagation was monitored by ^1H NMR (300.36 MHz) at 20°C, recording spectra with an interval of 12 to 24 h.

5.2.5.3 ROMP of DCPD (**Mon2**)



Scheme 15. ROM polymerization of DCPD (**Mon2**)

5 mL (36.95 mmol) of DCPD were filled into a 50 mL plastic tube and the required amount of initiator was injected (from a 4 mg/mL stock solution, topped up to 300 μ L) at approx. 33°C. Loadings (M:I) reached from 25000 to 300000, polymerizations were carried out at RT and 60°C in an oven. Polymerization progress was monitored by tipping into the tube with a spatula and noting the viscosity based on a scale reaching from 0 to 100 (see chapter 3.2.5.2).

5.2.5.4 Simultaneous Thermal Analysis (STA)

STA samples were prepared by mixing 1 mL of DCPD with a solution of the required amount of initiator (40 ppm, extracted from a stock solution) topped up to 60 μ L. Due to the very latent behaviour of the initiators at room temperature a shock freezing in liquid nitrogen of the samples was not necessary. About 13 mg of the mixture were transferred into a DSC pan which was immediately subjected to the STA run. The results of this analysis are presented in chapter 3.2.5.3.

Appendix

List of Abbreviations

bz	benzyloxy (OCH ₂ (C ₆ H ₅))
Cy	cyclohexane
DCPD	dicyclopentadiene
DME	dimethoxy ethane
DSC	differential scanning calorimetry
eq	equivalent
EtOAc	ethyl acetate
GPC	gel permeation chromatography
H ₂ IMes	1,3-bis(mesityl)-4,5-dihydroimidazol-2-ylidene
HSQC	Heteronuclear single quantum correlation spectroscopy
M	mol / L
MeOH	methanol
M:I	monomer to initiator ratio
NHC	N-heterocyclic carbene
NMR	nuclear magnetic resonance
NOESY	Nuclear Overhauser effect spectroscopy
<i>p</i> DCPD	<i>poly</i> (dicyclopentadiene)
py	pyridine
RT	room temperature
Ru	ruthenium
SIMes	saturated imidazol mesityl
STA	simultaneous thermal analysis
TGA	thermogravimetric analysis
THF	tetrahydrofuran
TLC	thin layer chromatography

List of Figures

Figure 1. Most prominent commercially available initiators used in olefin metathesis	10
Figure 2. Well-defined latent initiators	11
Figure 3. Chelating carbene ligand in the synthesized ruthenium complexes	12
Figure 4. ^1H NMR spectrum of the side product (300 MHz, CDCl_3)	18
Figure 5. Characteristic ^1H NMR spectrum of a vinyl compound (L1 , 300 MHz, CDCl_3)	19
Figure 6. ^1H NMR spectra of complex 2 (300 MHz, CDCl_3).....	22
Figure 7. ^1H NMR spectrum of the cationic side product (2a) (300 MHz, CDCl_3)	23
Figure 8. ^1H NMR spectrum of complex 2b (300.36 MHz, methanol- d_4).....	24
Figure 9. NHC ligand (H_2IMes) with highlighted protons.....	26
Figure 10. Comparison of the H_2IMes proton resonances (300.36 MHz) in the complexes 2, 2a (CDCl_3) and 2b (methanol- d_4), (crossed out peaks in 2a originate from free H_2IMes molecules)	26
Figure 11. Molecular structure of complex 1- CH_2Cl_2 (hydrogen atoms are hidden due to better clarity).....	27
Figure 12. Molecular structure of complex 3- $(\text{CDCl}_3)_3$ (hydrogen atoms are hidden due to better clarity).....	27
Figure 13. Complex A (<i>cis</i> -dichloro(2-formylbenzylidene- $\kappa^2(\text{C},\text{O})$)(1,3-bis(2,4,6-trimethylphenyl)-	28
Figure 14. Time/conversion plot of polymerizations in NMR tube.....	32
Figure 15. Carbene and aldehyde proton resonances during the ROM polymerization progress of Mon1 with initiator 2 and assumed decomposition compound (300 MHz, CDCl_3)	33
Figure 16. Comparison of the GPC results of Poly1, catalyzed with A, and 1-4 at different conditions.....	37
Figure 17. Polymerization progress of monomer 2 at RT (initiator loading = 40 ppm)	40
Figure 18. Polymerization progress of monomer 2 at 60°C (initiator loading = 40 ppm).....	40
Figure 19. Polymerization performance of initiator 1 at RT (comparison of all loadings).....	41
Figure 20. Comparison of the polymerization performance at RT (loading = 40 ppm).....	42
Figure 21. Comparison of the polymerization performance at 60°C (loading = 40 ppm)	42

Figure 22. DSC and TGA diagrams for ROMP of DCPD with initiator 2 (40 ppm, heating rate 3°C/min)	44
--	----

List of Schemes

Scheme 1. General reaction scheme for the synthesis of dichloro-ruthenium complexes.....	9
Scheme 2. Ring opening metathesis polymerization of DCPD.....	13
Scheme 3. Mechanism of transition metal olefin metathesis	14
Scheme 4. Dissociative (D) and associative (A) pathway for coordination of the alkene substrate (S)	15
Scheme 5. Two-step synthesis for the preparation of ligands L1-L4	17
Scheme 6. Synthesis of ruthenium complexes 1-4 starting from M31 ([1,3-bis(2,4,6-trimethylphenyl)-2-imidazolidinylidene]dichloro(3-phenyl-1H-inden-1-ylidene)(pyridyl)ruthenium(II))	21
Scheme 7. Polymerization procedure of <i>endo/exo</i> -dimethyl-bicyclo[2.2.1]hept-5-ene-2,3-dicarboxylate (Mon1)	31
Scheme 8. Possible pathway to the active species	34
Scheme 9. ROMP of Dicyclopentadiene (Mon2).....	38
Scheme 10. Reaction scheme for the esterification of the hydroxy group	49
Scheme 11. Reaction scheme for the etherification of the hydroxy group.....	51
Scheme 12. Reaction scheme for the Suzuki coupling reaction ⁹	54
Scheme 13. Synthesis of Ru(II)-complexes from M31	58
Scheme 14. ROM Polymerization of dimethyl-5-norbornene-2,3-dicarboxylate (Mon1).....	64
Scheme 15. ROM polymerization of DCPD (Mon2)	65

List of Tables

Table 1. Ligands used for initiator synthesis	20
Table 2. Esters (ligand precursors)	20
Table 3. <i>Cis</i> -dichloro ruthenium complexes.....	25
Table 4. Selected bond lengths of complexes 1, 3 and A (Å)	28
Table 5. Selected bond angles of complexes 1, 3 and A (°)	29
Table 6. Results of the solubility test	30
Table 7. Reaction conditions and GPC results of Poly1.....	36
Table 8. Scale to estimate the viscosity and hence the polymerization progress	39
Table 9. Results of STA for Initiators 1-4 and A (reference).....	44